7-17-1965

A modified electron optical system and the gamma-electron angular correlation of gold-198.

Murray Lawrence Trudel
University of Windsor

INFORMATION TO USERS

This manuscript has been reproduced from the microfilm master. UMI films the text directly from the original or copy submitted. Thus, some thesis and dissertation copies are in typewriter face, while others may be from any type of computer printer.

The quality of this reproduction is dependent upon the quality of the copy submitted. Broken or indistinct print, colored or poor quality illustrations and photographs, print bleedthrough, substandard margins, and improper alignment can adversely affect reproduction.

In the unlikely event that the author did not send UMI a complete manuscript and there are missing pages, these will be noted. Also, if unauthorized copyright material had to be removed, a note will indicate the deletion.

Oversize materials (e.g., maps, drawings, charts) are reproduced by sectioning the original, beginning at the upper left-hand corner and continuing from left to right in equal sections with small overlaps.

UMI®

.

A MODIFIED ELECTRON OPTICAL SYSTEM

AND THE $\gamma - e^-$ ANGULAR CORRELATION

OF Au^{198}

BY

MURRAY LAWRENCE TRUDEL

A Thesis
Submitted to the Faculty of Graduate Studies through the
Department of Physics in Partial Fulfillment
of the Requirements for the Degree of
Master of Science at
The University of Windsor

Windsor, Ontario

1965

UMI Number:EC52587

UMI®

ProQuest Information and Learning Company
789 East Eisenhower Parkway
P.O. Box 1346
Ann Arbor, MI 48106-1346

ABM 6513

APPROVED:
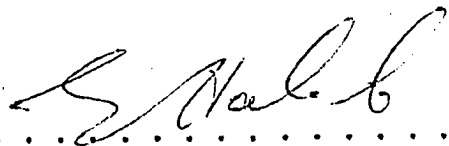
. . . .
E. E. Habib

. . . .
F. Holuj

. . . .
S. Kalra

120922

ABSTRACT

The electron optics used in angular correlation measurements were modified in order to measure both the A_2 and the A_4 correlation coefficients of the correlation function:

$$W(\omega) = \sum_{K} A_{2K} \, P_{2K} \, (\cos \omega)$$

A new experimental method for the study of the electron conversion process involving the b_2 particle parameter is outlined.

The modified optics system was employed in a $\gamma - e^-$ directional correlation experiment for the $2^+ \longrightarrow 2^+ \longrightarrow 0^+$ cascade in $_{79}Au^{198}$. The results of the experiment were analysed according to the new method above.

From this experiment, the value of the b_2 particle parameter obtained was:

$$b_2 = 1.19 \pm 0.10$$

This result agrees with the theoretical calculation of b_2 obtained by Biedenharn and Rose (1953) within the limits of experimental error.

ACKNOWLEDGEMENTS

I would like to express my appreciation to Dr. E. E. Habib for his guidance and instruction throughout this work.

My thanks go to Mr. W. Grewe for the part he played in the construction of the modified electron optics system. I would like to thank Miss Linda Cummings for typing the manuscript. I am indebted to the Government of Ontario for financial support in the form of a bursary.

iii

TABLE OF CONTENTS

LIST OF TABLES

vi

LIST OF ILLUSTRATIONS

CHAPTER I

ANGULAR CORRELATIONS IN NUCLEAR SPECTROSCOPY

(i) Introduction

If a nucleus undergoes emission of two radiations in succession (nuclear α, β, or γ - radiation, or secondary radiations from the surrounding electron shells), their correlations are an attractive and useful field of study. Such studies can be divided into essentially two kinds: spatial correlations and time correlations. The first ones (angular correlations) constitute the topic of this chapter. For completeness, however, it may be said that time correlations studies concern the time delay between the two transitions (delayed coincidences) and that in many cases, the purpose of these studies is the determination of the coincidence intensity of two kinds of transitions, i.e. the number of transitions of the first kind following (or preceding) the other in the construction of decay schemes. Often, only a very rough knowledge of coincidence intensities is necessary for this last purpose.

(ii) Angular Correlation of Successive Radiations

The photons emitted by a sample in which a large number of nuclei are undergoing identical γ - ray transitions will be isotropic in the laboratory coordinates. There is no preferred direction of emission for the γ - ray photon from the individual transition $I_a \xrightarrow{\gamma} I_b$ because the atoms and nuclei are oriented at random. The same is true for α - ray, β - ray and conversion electron emission. If the transition $I_a \longrightarrow I_b$ is followed by a second transition $I_b \longrightarrow I_c$, the individual radiations from the second transition are likewise isotropic in the laboratory coordinates.

1

However, in a two step cascade transition, such as

$I_a \xrightarrow{\gamma_1} I_b \xrightarrow{\gamma_2} I_c$ there is often an angular correlation between

the directions of emission of two successive γ - ray photons γ_1, and γ_2,

which are emitted from the same nucleus. Often there are similar angular

correlations for other pairs of successive radiations, such as $\alpha-\gamma$,

$\beta-\gamma$, $\beta-e^-$ (where e^- means a conversion electron), $\gamma-e^-$, ...

The existence of an angular correlation arises because the

direction of the first radiation is related to the orientation of the

angular momentum I_b of the intermediate level. This orientation can be

expressed in terms of the magnetic angular momentum quantum number m_b

with respect to some laboratory direction such as that of the first radiation.

If I_b is not zero, and if the lifetime of the intermediate level is short

enough so that the orientation of I_b persists, then the direction of emission

of the second radiation will be related to the direction of I_b and hence to

that of the first radiation.

(iii) The Purpose of Angular Correlations

The angular correlation of radiations emitted or absorbed in

nuclear processes has been one of the principal tools available for the

nuclear spectroscopy of excited states.

The information that can be obtained from angular correlation

work depends on the type of radiation observed (α, β, γ, e^-), on the

properties that are singled out by the experiment (direction, polarization,

energy), and on the extranuclear fields acting on the nucleus.

If we assume that the decaying nuclei are free, i.e. that no

extranuclear fields act on the nucleus and disturb its orientation in the

intermediate state, then, to the extent that this can be realized in practice,

angular correlation measurements provide information about the properties of

the nuclear levels involved and about the angular momenta carried away by the

radiations. To be more precise, $\alpha-\gamma$ and $\gamma-\gamma$ directional correlations yield the spins of the nuclear levels, but not the parities. The relative parities can be determined, however, if one observes in addition to the direction, the polarization of the γ - rays, or if one measures the directional correlation between conversion electrons (e^-). $e^- - \gamma$ correlations provide new information concerning the details of nuclear structure, viz, the newly discovered "nuclear penetration matrix elements" [Church and Weneser, (1956)]. Angular correlations that involve either the polarization of β - particles or the circular polarization of γ - rays, yield information on the interaction in β - decay.

The information that can be obtained from the influence of extranuclear fields on the nuclear angular correlation is also multifold. Very often, one can determine the quadrupole coupling from the change of the correlation due to extranuclear fields. In many cases, one can measure the g - factor of an excited nuclear state by observing the directional correlation as a function of an external magnetic field. From the g - factor one gets the magnetic moment if the spin of the nuclear state is known, e.g. from the unperturbed directional correlation.

The above specified information by no means exhausts the vast amount of knowledge obtainable from angular correlations. Further elaboration, however, is beyond the scope of this work.

(iv) Theory of Angular Correlations

(a) Introduction

The theory of angular correlation is highly developed and general expressions can be written down for even very complex situations. However, the general formulation of the theory is very complicated and is somewhat lengthy. Very good formulations of the theory are present in the literature

[Biedenharn and Rose, (1953)]. We will therefore present in this section a simple treatment of directional correlation that, while restricted in its usefulness, provides some insight into the correlation mechanism.

The common feature of all correlation problems is to be found in the fact that they involve an initial nuclear state of sharp angular momentum I_1 and parity that undergoes successive transformations either emitting or absorbing radiations through intermediate nuclear states of sharp angular momenta I_a, I_b .... with sharp parity and terminating as a nucleus with sharp angular momentum I_2 and parity. This assumption of sharp angular momenta and parity is restrictive and distinguishes the correlation problem from say the closely related problem of the angular distribution of nuclear reactions which show coherent mixing of the intermediate nuclear states.

(b) The Theoretical Directional Correlation Function

The schematic picture of a directional correlation measurement is shown in Figure 1.1. A nuclear cascade involving states a, b, c with spins I_a, I_b, I_c occurs through the successive emission of particles (or photons) R_1 and R_2 (It is assumed here that the spins and parities of the states a, b, c are well defined).

The most convenient form in which to express the correlation function $W(\Theta)$ is:

$$W(\Theta) = \sum_{K=0}^{K_{max.}} A_K P_K (\cos \Theta) \tag{1.1}$$

The functions P_K are Legendre polynomials. The coefficients A_K contain all the physical information. Usually one chooses $A_0 = 1$, so that the correlation function integrated over all angles is unity:

$$\int W(\Theta) \, d\Omega = 1 \tag{1.2}$$
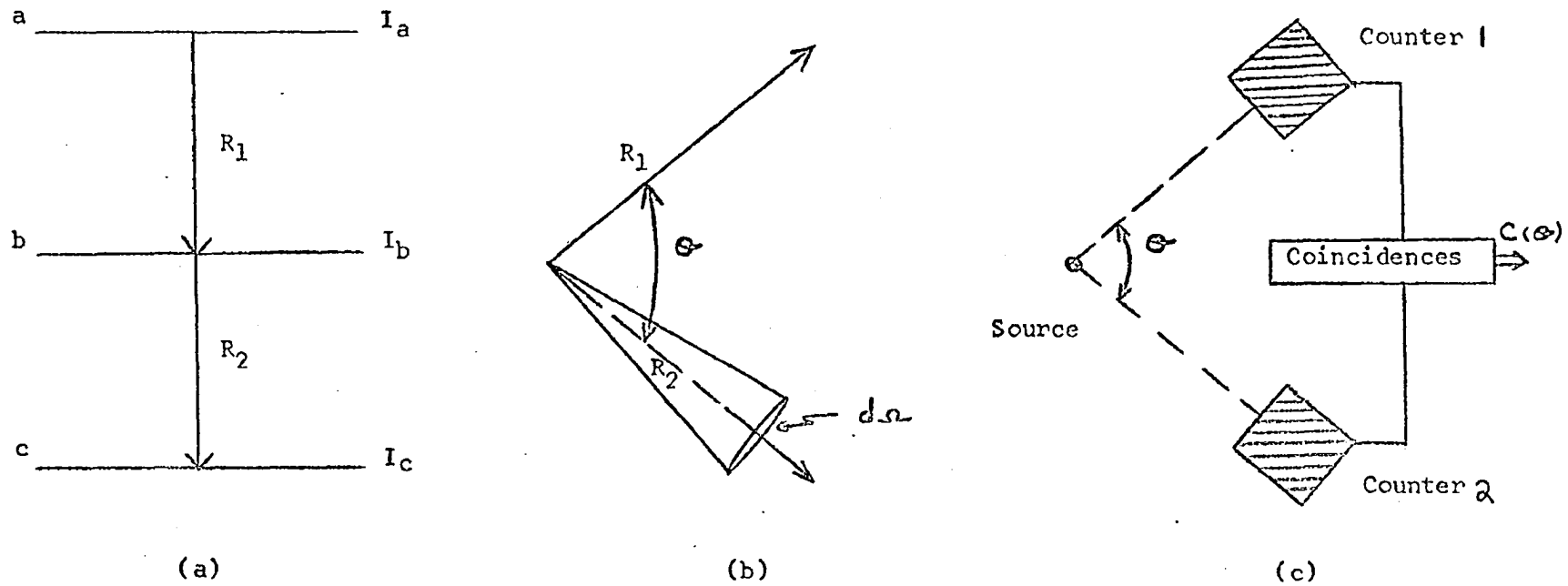
Figure 1.1   Schematic of a Directional Correlation Measurement

(a) Nuclear cascade

(b) $W(\theta)\,d\Omega$ is the relative probability that the radiation R_1 is emitted into the solid angle $d\Omega$ at an angle θ with respect to R_2.

(c) The two counters 1 and 2 subtend an angle θ at the source. From the coincidence count rate as a function of angle, $C(\theta)$, one obtains after suitable correction the correlation function $W(\theta)$.

At this point we introduce the following nomenclature for a double cascade, viz, I_a (L_1) I_b (L_2) I_c where I_a, I_b and I_c denote the angular momenta of the first, intermediate and final nuclear levels, and L_1, and L_2 are the angular momenta of the two successive radiations.

Three general rules for the coefficients A_K hold for all types of particles:

$$K \text{ integer, even} \tag{1}$$

$$0 \leq K_{max.} \leq \text{min.} (2I_b, 2L_1, 2L_2) \tag{2}$$

$$A_K = A_K (a,b) A_K (b,c) \tag{3}$$

Rule 1 expressing the fact that only even Legendre polynomials appear, holds as long as one measures only directions and linear polarizations of the radiations. The observation of the circular polarization, however, introduces also odd integers.

Rule 2 states that the highest term $K_{max.}$ in the expansion is smaller than, or equal to, the smallest of the three numbers $2I_b$, $2L_1$, $2L_2$ where L_1 and L_2 are the angular momenta carried away by R_1 and R_2. This rule implies isotropic correlation if the angular momentum of either of the radiations or of the intermediate state equals 0 or 1/2.

Rule 3 expresses the fact that the coefficients A_K for a cascade can be broken up into two factors, each factor depending on only one transition of the cascade. The second factor A_K (b,c) for instance is entirely determined by the properties of the levels b and c and the radiation R_2.

Equation 1.1 is very general indeed, and with the proper evaluation of A_K it applies to all two step cascades $\alpha - \gamma$, $\beta - \gamma$, $\gamma - \ell^-$, $\ell^- - \ell^-$, etc. as well as to nuclear scattering experiments and nuclear disintegrations.

Numerical values for the factors A_K (a,b) for given properties of the levels (a) and (b) and of the radiation R have been calculated and tabulated for most cases of interest.

As an example of the above, consider the directional correlation between successive gamma rays in the cascade shown in Figure 1. 2(a) ($I_a = 2^+$, $I_b = 2^+$, $I_c = 0^+$). The second gamma ray in this cascade must be pure quadrupole, and from the references in the literature, we find the corresponding directional correlation factors A_2 (b,c) = -0.5976, A_4 (b,c) = -1.069. If we assume the first transition to be pure also, for instance dipole radiation ($L_1 = 1$), we find immediately A_2 (a,b) = -0.4183 and A_4 (a,b) = 0 and hence A_2 = 0.2500 and A_4 = 0. These values have to be compared with experiment.

Generally, however, the first transition in a $2^+ \Rightarrow 2^+ \Rightarrow 0^+$ cascade will be mixed, i.e. the radiation carried away involves more than one single value of angular momentum. Angular momentum selection rules allow L_1 = 1,2,3 or 4. As a rule only the two lowest multiples, L_1 = 1, and L_1' = 2, occur with measurable intensity [cf. Figure 1.2(b)]. The coefficients A_2 (a,b) and A_4 (a,b) and hence also A_2 and A_4 now become continuous functions of the mixing ratio δ, which in this case indicates the ratio of amplitude of the quadrupole to that of the dipole contribution (δ^2 is defined as the ratio of the total intensity of the L' pole to that of the L pole).

The most convenient representation of the dependence of A_2 and A_4 on δ is a parametric plot [Coleman, (1958)]: one draws the curve $A_2 = A_2$ (δ), $A_4 = A_4$ (δ) in an $A_2 - A_4$ plane [The functions A_2 (δ) and A_4 (δ) are calculated from the formulas and coefficients by Frauenfelder (1955), Biedenharn and Rose (1953), Ferentz and Rosenzweig
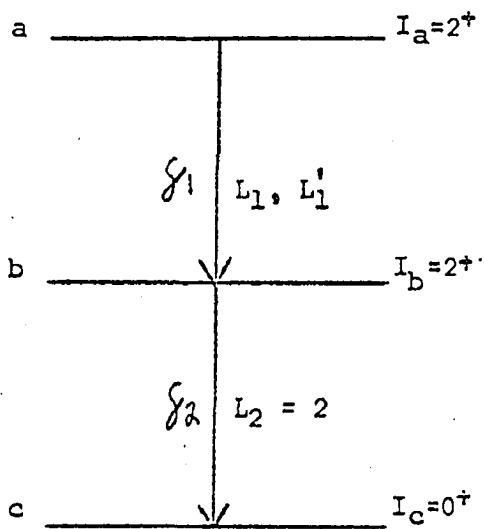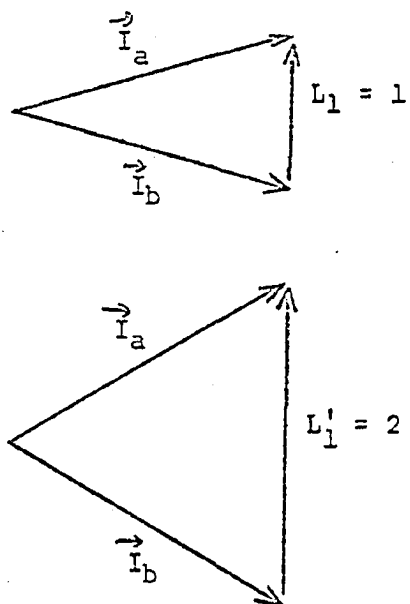
Figure 1.2   A γ-γ cascade.

(a) $2^+ \longrightarrow 2^+ \longrightarrow 0^+$ cascade (where the superscript + denotes even parity), occurring frequently in even-even nuclei.

(b) The first gamma ray γ_1 is usually mixed in this case; the two dominant angular momenta being $L_1 = 1$, $L_1' = 2$.

(1955), and Arns and Wiedenbeck (1958)]. A parametric plot for the cascade $2^+ \longrightarrow 2^+ \longrightarrow 0^+$ is shown in Figure 1.3. The experimental points with coordinates $A_{2,exp.}$ and $A_{4,exp.}$ must lie on this curve and thus yield values for sign and magnitude of the mixing ratio δ.

(v) Particle Parameters

At this point we recall the form of the A_K coefficients, viz, $A_K = A_K (a,b) A_K (b,c)$. From the theory of angular correlations it may be shown [Biedenharn and Rose, (1953)] that the individual factors $A_K (a,b)$ and $A_K (b,c)$ also factor into two separate factors namely into a "nuclear factor" which depends on specific nuclear properties, and a "geometrical factor" which describes the geometry of the problem.

It is convenient to adopt the $\gamma - \gamma$ angular correlation function as the standard representation of the "geometry" of the correlation process and to express the angular correlation for different radiations by defining a multiplicative particle parameter b_K to effect the necessary change from the standard correlation. Of course, the choice of the $\gamma - \gamma$ correlation as the standard one is arbitrary. We could have chosen the $\alpha - \alpha$ correlation which, from the point of view of analytical simplicity and availability of numerical results, would have been almost equally suitable. However, the fact that the parity restriction precludes the mixing of even and odd L militates against this choice. For γ-rays the parity for given L depends on the character of the radiation (electric or magnetic) and mixtures of all L, L' pairs (consistent with angular momentum conservation) are permissible in principle.

Particle parameters b_K may be introduced to express the angular correlation between any two successive radiations. The detailed information obtainable from the use of these parameters is beyond the scope of this work.
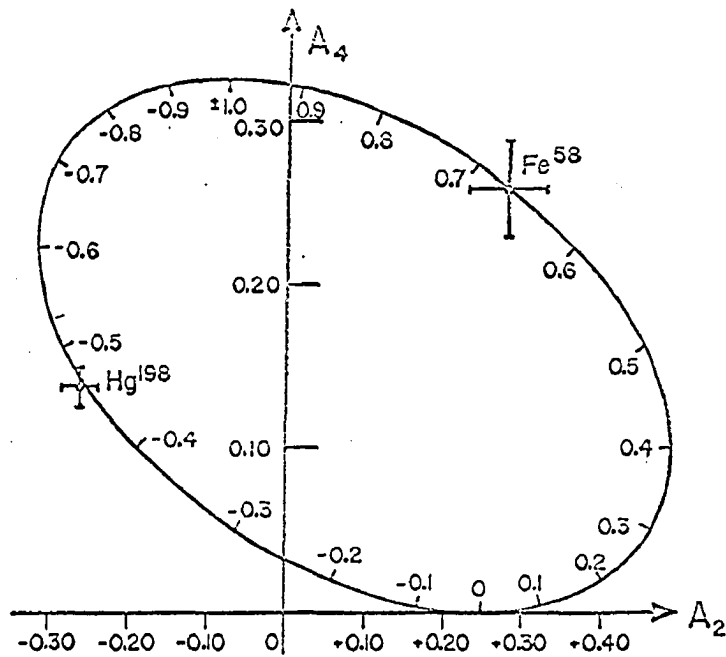
Figure 1.3   A parametric plot.

Parametric plot of the directional correlation coefficients

A_2 and A_4 for the cascade $2^+ \longrightarrow 2^+ \longrightarrow 0^+$. δ is

the mixing ratio (quadrupole to dipole radiation) in the first

transition. The curve is labeled with the values of the

parameter $\delta' = \dfrac{\delta}{1 - |\delta|}$. Two experimental points are shown.

Of particular interest to us here is the $\gamma - e^-$ angular correlation since the experiment performed in this thesis was the 679 Kev γ - 412 Kev e^- angular correlation in Au^{198}. A new experimental technique involving the b_K particle parameters was employed.

<u>(vi) The New Technique</u>

(a) Introduction

A new experimental technique for the study of the internal conversion process has been developed. The new method implies an indirect and accurate determination of the particle parameter b_2 from an experimental measurement of the b_4 particle parameter. It is shown that the accuracy in the value for b_2 thus obtained is considerably higher than would be possible on the basis of a direct measurement of b_2. On the basis of the theory of Green and Rose (1958), the parameter b_2 when accurately determined, may be used to derive experimental values for any dynamic contributions to the conversion process if they are present. However, to be decisive for this analysis b_2 has to be known to within a few percent. An experimental accuracy of this order has so far not been possible to achieve.

(b) The New Method For Accurate b_2 Determinations

The usual expansion of the correlation function $W(\theta)$ in terms of Legendre polynomials, reads, in the case of gamma - gamma directional correlations:

$$W(\theta, \gamma\gamma) = \sum_K A_{2K}(\gamma\gamma) P_{2K}(\cos\theta) \qquad (1.3)$$

For pure gamma - electron ($\gamma - e^-$) correlations a similar expansion applies:

$$W(\theta, \gamma e^-) = \sum_K A_{2K}(\gamma e^-) P_{2K}(\cos\theta)$$
$$= \sum_K b_{2K} A_{2K}(\gamma\gamma) P_{2K}(\cos\theta) \qquad (1.4)$$

Thus from a study of the gamma – electron and gamma – gamma correlations measured with the same source and under identical experimental conditions we obtain:

$$b_2 = \frac{A_2(\gamma e^-)}{A_2(\gamma \gamma)} \qquad (1.5)$$

$$b_4 = \frac{A_4(\gamma e^-)}{A_4(\gamma \gamma)} \qquad (1.6)$$

This comparison method has the additional advantage that the particle parameters determined by (1.5) and (1.6) are unaffected by all attenuations caused by extra-nuclear fields since the attenuation coefficients if present disappear in the ratios.

The value for b_2 thus obtained cannot be sufficiently accurately determined to be of significance for analysis of dynamic effects. However, the two particle parameters are not mutually independent. As shown by Biedenharn and Rose (1953) b_2 and b_4 are inter-related by means of a recursion formula. In this particular case, with the numerical constants introduced, the recursion formula reads:

$$b_2 = 1.4 - \frac{b_4}{2.5} \qquad (1.7)$$

Consequently we may use our experimentally determined b_4 value to derive a corresponding value for b_2. Moreover, because of the appearance of the numerical factors 1.4 and the 2.5 in the denominator the relative error in b_2 is considerably smaller than the corresponding error in b_4. Thus, provided b_4 can be measured with a reasonable degree of accuracy, the corresponding value for b_2 will be quite precisely determined. This condition is fulfilled whenever $A_4(\gamma \gamma)$ is sufficiently large which

is the case for the 679 Kev - 412 Kev gamma gamma cascade in Au^{198}.

This indirect way to arrive at a b_2 value from a measurement of b_4, results in an accuracy which is considerably higher than is possible to achieve in any direct determination of b_2 from the measured A_2 ($\gamma\gamma$) and A_2 ($\gamma \alpha^-$).

CHAPTER II

CORRECTIONS FOR FINITE SOLID ANGLE

(i) Corrections for the Gamma Channel

The coincidence counting rate per unit solid angle $\sin\theta\, d\theta\, d\varphi$

(where the angles represent the relative orientation of the propagation

vectors of the two radiations) for an angular correlation measurement

is proportional to:

$$W(\theta) = \sum_{K=0}^{K_{max.}} A_{2K}\, P_{2K}(\cos\theta) \qquad\qquad (2.1)$$

The measured correlation, however, is less than the true correlation

because of the finite solid angle that the two detectors must subtend in

any feasible experiment.

When the detectors for the two radiations subtend finite solid

angles Ω_1 and Ω_2 at the source, it is advisable to modify the theoretical

correlation and compare this smeared correlation with the measured one.

The geometry envisaged is shown in Figure 2.1. The detectors (scintillation

counters) are assumed to be crystals cut in the form of right circular

cylinders with the base oriented towards the source. The source, at the

origin, is on the intersection of the axes of the cylinders. In this case,

as the following shows, the form of the correlation function is unchanged

and each coefficient A_{2K} becomes multiplied by an attenuation factor for

which one can obtain an exact and very simple expression. Taking into

account the absorption of the radiation in each crystal, we introduce the

following notation. The distance from the source to the front face of each

crystal is h, the thickness is t, and r is the radius of the crystal. If

x(B) is the distance traversed by the radiation incident on the crystal at

an angle B with the axis, the absorption is proportional to $(1 - e^{-\tau x(B)})$

where τ is the absorption coefficient. Then the measured correlation

14
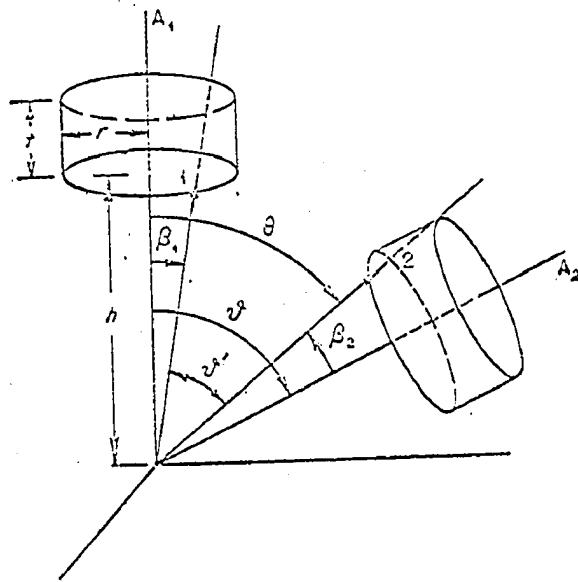
Figure 2.1   A geometry of two γ detectors.

Geometry for finite resolution in angular
momentum. The notation applies for singles
counts as in angular distribution measurements.
The azimuth angles φ_1 and φ_2 are measured with
respect to the cylinder axes A_1 and A_2 respectively.

function would be:

$$\overline{W}(\theta) = \frac{\int d\Omega_1 \, d\Omega_2 \, W(\theta')(1-e^{-\tau x_1})(1-e^{-\tau x_2})}{\int d\Omega_1 \, d\Omega_2 \, (1-e^{-\tau x_1})(1-e^{-\tau x_2})} \qquad (2.2)$$

where x_1 and x_2 refer to the two crystals, $d\Omega_1$ and $d\Omega_2$ are the solid angle elements for each radiation, and θ' is the angle between their propagation vectors, while θ is the angle between the cylinder axes.

The required integrals are of the form:

$$I_\ell = \int d\Omega_1 \, d\Omega_2 \, P_\ell(\cos\theta')(1-e^{-\tau x_1})(1-e^{-\tau x_2}) \qquad (2.3)$$

which by application of the Legendre polynomial addition theorem reduces to:

$$I_\ell = 4\pi^2 P_\ell(\cos\theta) \, J_\ell(1) \, J_\ell(2) \qquad (2.4)$$

where

$$J_\ell = \int_0^\beta P_\ell(\cos\beta)(1-e^{-\tau x(\beta)}) \sin\beta \, d\beta \qquad (2.5)$$

β being the half angle subtended on the front face, and (1) and (2) refer to the respective crystals. We have to evaluate J_ℓ to obtain the required correction factors. Finally, we have:

$$W(\theta) = 1 + \left(\frac{J_2(1)}{J_0(1)}\right)\left(\frac{J_2(2)}{J_0(2)}\right) A_2 P_2(\cos\theta)$$

$$+ \left(\frac{J_4(1)}{J_0(1)}\right)\left(\frac{J_4(2)}{J_0(2)}\right) A_4 P_4(\cos\theta) \qquad (2.6)$$

The attenuation factor is:

$$f_2(\gamma\gamma) = \left(\frac{J_2}{J_0}\right)^2 \qquad (2.7)$$

for similar detectors, and for γ-rays with similar absorption coefficients. For a single detector as would be used in an angular distribution measure, with the data represented by equation 1.1, the attenuation factor would be simply:

$$f_2(\gamma) = \frac{J_2}{J_0} \qquad (2.8)$$

Values for J_2/J_0 and J_4/J_0 have been calculated (Figures 2.2 and 2.3) by West (1959) for crystal sizes of 1 1/2 inches in diameter by 1 inch long, 1 3/4" x 2", 2" x 2", and 3" x 3" for source to crystal face distances of 3,5,7 and 10 cm.

In the γ-e^- correlation experiment to be described (Chapter V) a 2" x 2" crystal and a 1 3/4" x 2" crystal were utilized at a distance of 10 cm. from the source. The graphs (Figures 2.2 and 2.3) then yield the following values for the correction factors:

$$f_2(\gamma) = \frac{J_2}{J_0} \quad = \quad 0.965$$

for 2" x 2" crystal

$$f_4(\gamma) = \frac{J_4}{J_0} \quad = \quad 0.886$$

$$f_2(\gamma) = \frac{J_2}{J_0} \quad = \quad 0.973$$

for 1 3/4" x 2" crystal

$$f_4(\gamma) = \frac{J_4}{J_0} \quad = \quad 0.912$$
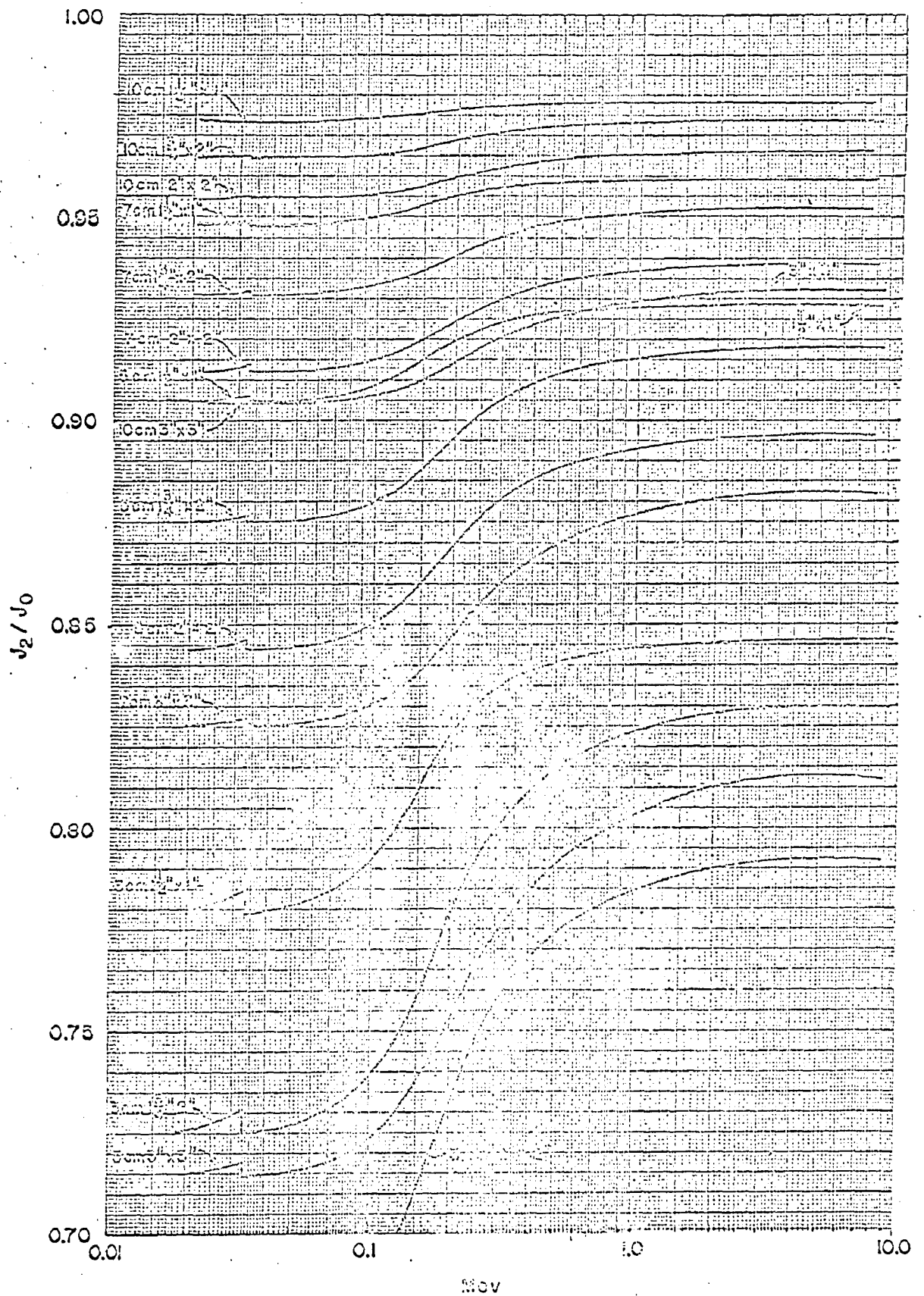
Figure 2.2
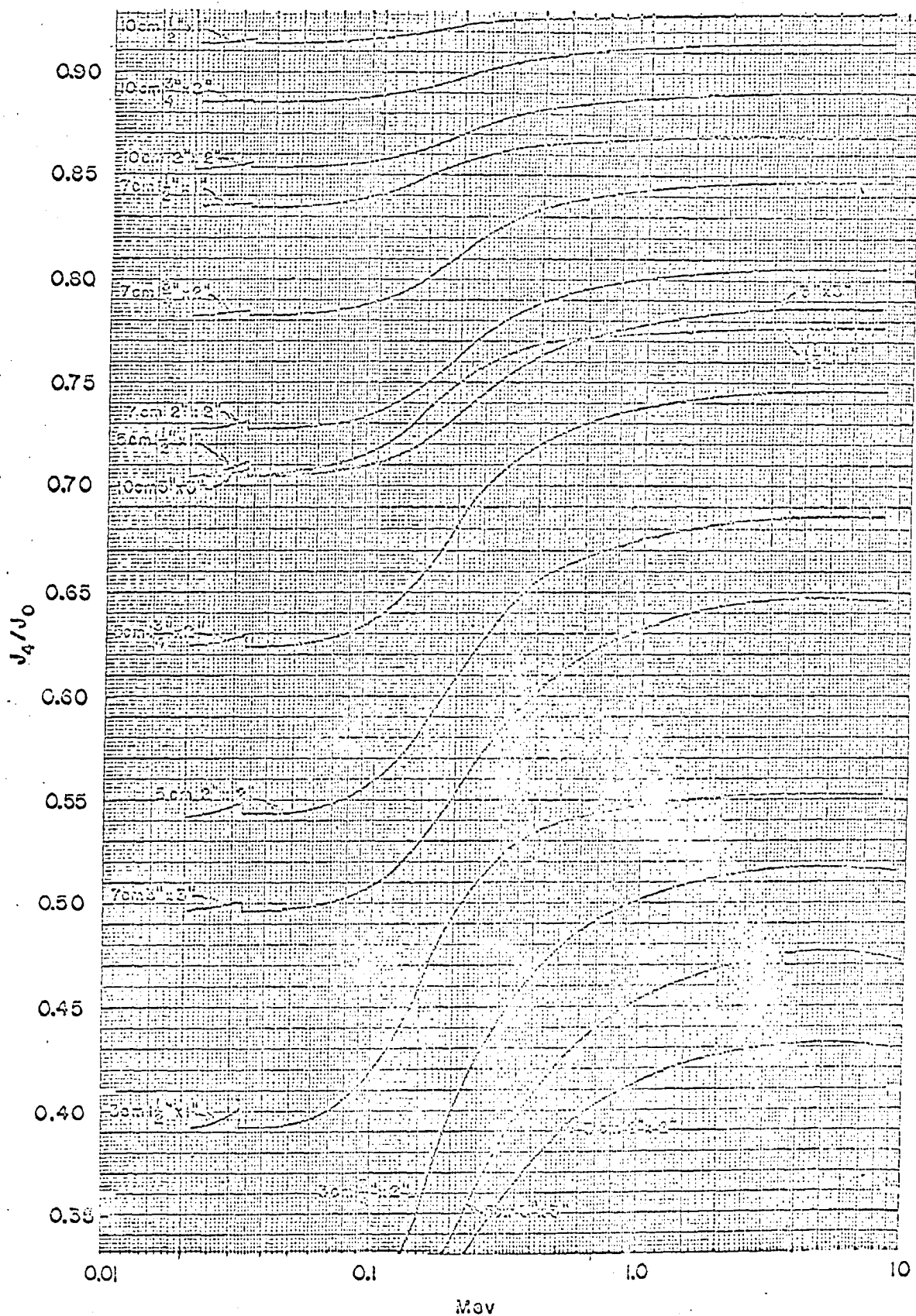
Figure 2.3

(ii) Corrections for the Electron Channel

Apart from the $\left(J_\ell / J_o\right)$ correction factors for the γ — channel discussed above, we have in the case of an electron correlation, also to apply due corrections for the smearing out of the directional correlation owing to the finite aperture angle subtended by the accepted cone of electrons in the beta spectrometer.

In this case, the form of the ℓ^-– correction factor, denoted $f_\ell(\ell^-)$, is similar to the previously discussed γ-correction factor $f_\ell(\gamma)$ since the geometrical arrangements of detector and source in both cases are similar (compare Figures 2.4 and 2.1).

Then, for the ℓ^- channel the appropriate expression for $f_\ell(\ell^-)$ is given by:

$$f_\ell(\ell^-) = \frac{\int_{\alpha_1}^{\alpha_2} P_\ell(\cos\alpha)\, Q(\alpha)\, \sin\alpha \, d\alpha}{\int_{\alpha_1}^{\alpha_2} Q(\alpha)\, \sin\alpha \, d\alpha} \qquad (2.9)$$

where α_1 and α_2 represent the minimum and maximum electron take-off angles (Figure 2.4) and $Q(\alpha)$ is the detector efficiency for the emission angle α.

Equation (2.9) is to be compared with the expression for $f_\ell(\gamma)$, namely:

$$f_\ell(\gamma) = \frac{J_\ell}{J_o} = \frac{\int_0^{\bar{\beta}} P_\ell(\cos\beta)\left(1 - a^{-Tx(\beta)}\right)\sin\beta \, d\beta}{\int_0^{\bar{\beta}} \left(1 - a^{-Tx(\beta)}\right)\sin\beta \, d\beta} \qquad (2.10)$$

It is evident from a comparison of equations (2.9) and (2.10) and of Figures 2.1 and 2.4 that the expression $Q(\alpha)\sin\alpha$ in the ℓ^- case is equivalent to the expression $\left(1 - a^{-Tx(\beta)}\right)\sin\beta$ in the γ-case. Further, it is seen that the integration over α from $\alpha_1 \longrightarrow \alpha_2$ in the ℓ^- case is
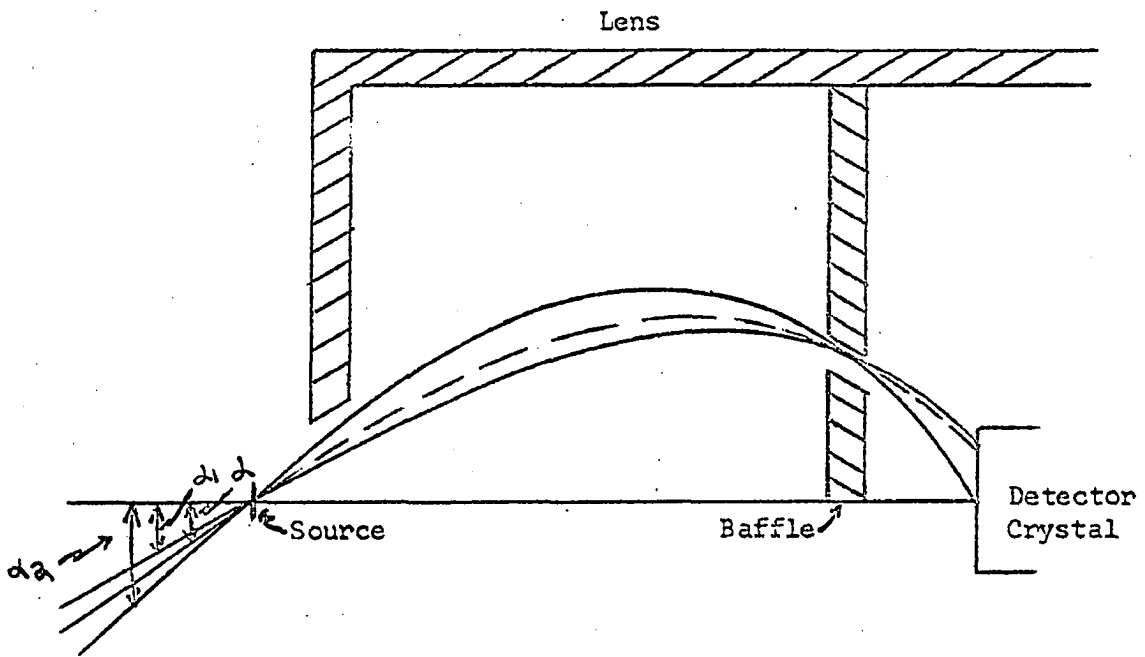
Figure 2.4   A geometry of an ℓ – channel.

equivalent to the integration over B from $0 \longrightarrow \beta$ in the ζ-case.

In general, then, the expression for the experimentally measured directional correlation becomes:

$$W(\Theta) = 1 + \mathcal{f}_2 A_2 P_2 (\cos \Theta) + \mathcal{f}_4 A_4 P_4 (\cos \Theta) \qquad (2.11)$$

where $\mathcal{f}_2$ and $\mathcal{f}_4$ are always $< |$ and represent the total smearing out of the angular correlation pattern due to the finite apertures in the two channels.

In particular, for an $\ell^- \zeta$ correlation:

$$\mathcal{f}_2 = f_2 (\ell^-) f_2 (\zeta) \quad < |$$
$$\mathcal{f}_4 = f_4 (\ell^-) f_4 (\zeta) \quad < | \qquad (2.12)$$

Returning to equation (2.9), it may be noted that for small transmission settings where α_1 is very nearly equal to α_2, we obtain:

$$\mathcal{f}_2 (\ell^-) \simeq P_2 (\cos \alpha)$$

i.e. $\qquad \mathcal{f}_2(\ell^-) \simeq P_2 (\cos \alpha) \qquad (2.13)$

$$\mathcal{f}_4 (\ell^-) \simeq P_4 (\cos \alpha) \qquad (2.14)$$

These functions (i.e. $P_2 (\cos \alpha)$ and $P_4 (\cos \alpha)$) are reproduced in Figure 2.5. At higher transmission settings the approximate relations (2.13) and (2.14) no longer apply. Both factors decrease, $\mathcal{f}_4$ more rapidly than $\mathcal{f}_2$ since the transmission increases with α_1 and larger α-values therefore dominate the contributions to the $\mathcal{f}_2$ and f_4 integrals, an effect which is more pronounced for the $\mathcal{f}_4$ factor than it is for the $\mathcal{f}_2$ factor. For this reason the experimentally measured $\mathcal{f}_2$ and f_4 factors at higher transmission settings no longer correspond to the geometrical mean value for α. We use, of course, our experimental values for $\mathcal{f}_2$ and $\mathcal{f}_4$.
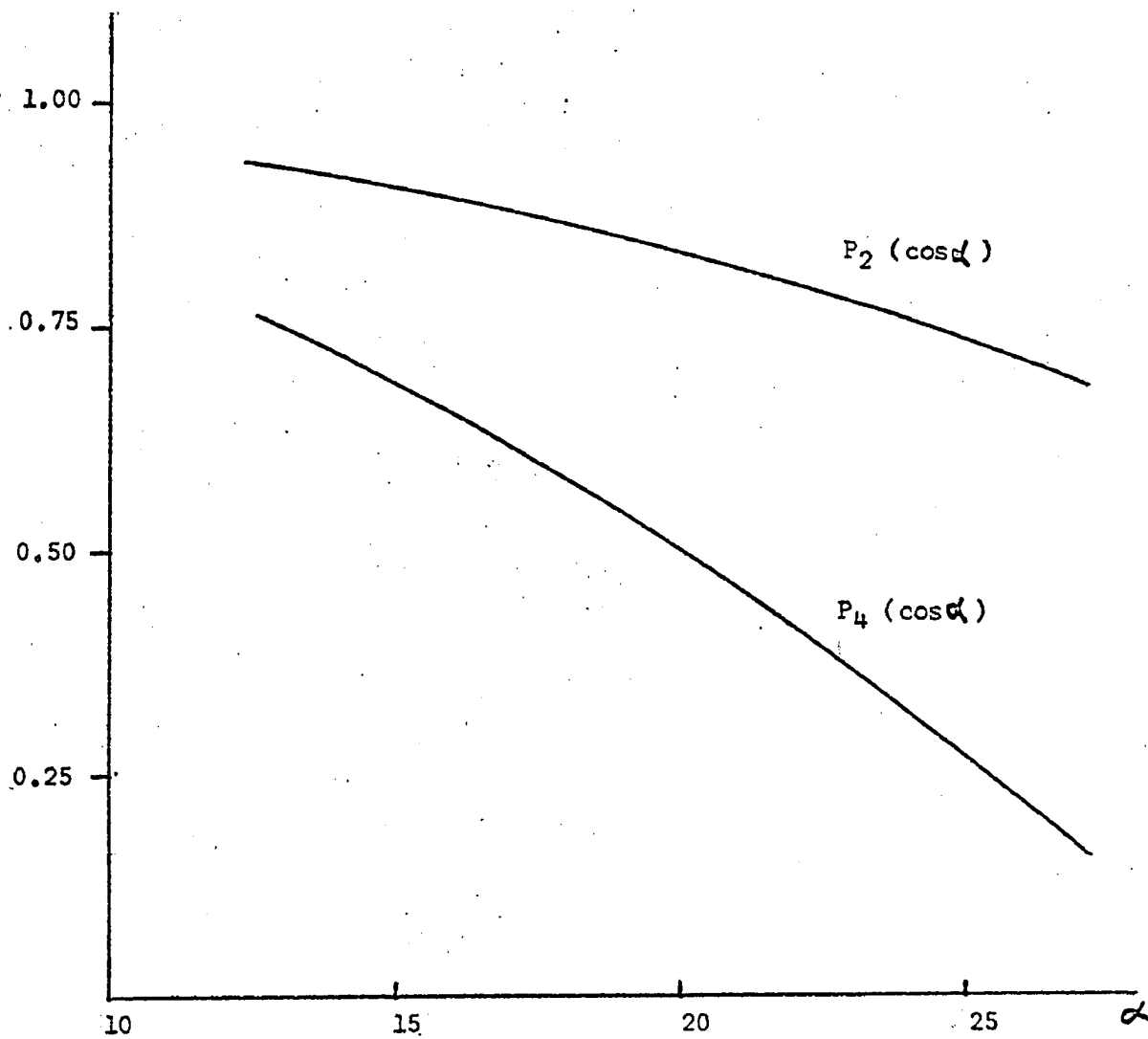
Figure 2.5   Graphs of $P_2 (\cos \alpha)$ and $P_4 (\cos \alpha)$.

(iii) The P_0, P_2, P_4 Baffles

Three special baffles, the so-called P_0, P_2 and P_4 baffles (Figure 2.6), are used to evaluate equations (2.8) and (2.9) experimentally.

The P_2 and P_4 baffles have been made such that they simulate a P_2 and a P_4 distribution respectively. The reduced counting rate therefore becomes a direct measure of the smearing out effects. The P_0 baffle is used, of course, for normalization. The P_4 baffle and the P_2 baffle have openings cut in them each of which has an area given by:

$$a_4 = K \int_{\alpha_1}^{\alpha_2} P_4(\cos \alpha) \sin \alpha \, d\alpha \qquad (2.15)$$

$$a_2 = K \int_{\alpha_1}^{\alpha_2} P_2(\cos \alpha) \sin \alpha \, d\alpha \qquad (2.16)$$

respectively, where K = constant, while the P_0 baffle has openings of area:

$$a_0 = K \int_{\alpha_1}^{\alpha_2} \sin \alpha \, d\alpha \qquad (2.17)$$

If the P_2 or P_4, and the P_0 baffles are now placed in turn at the spectrometer entrance, the count rates obtained will be proportional to the areas of the baffle openings. Hence:

$$\frac{N(P_2)}{N(P_0)} \simeq \frac{\int_{\alpha_1}^{\alpha_2} Q(\alpha) P_2(\cos \alpha) \sin \alpha \, d\alpha}{\int_{\alpha_1}^{\alpha_2} Q(\alpha) \sin \alpha \, d\alpha} = f_2(\alpha) \qquad (2.18)$$

P₂ Baffle

(b)

Figure 2.6

P₀ Baffle

(a)
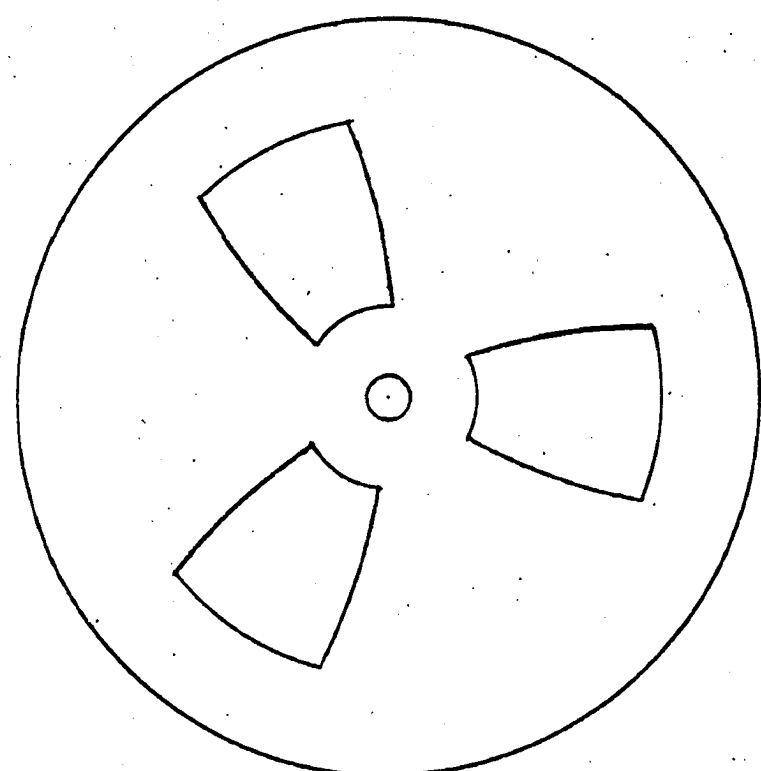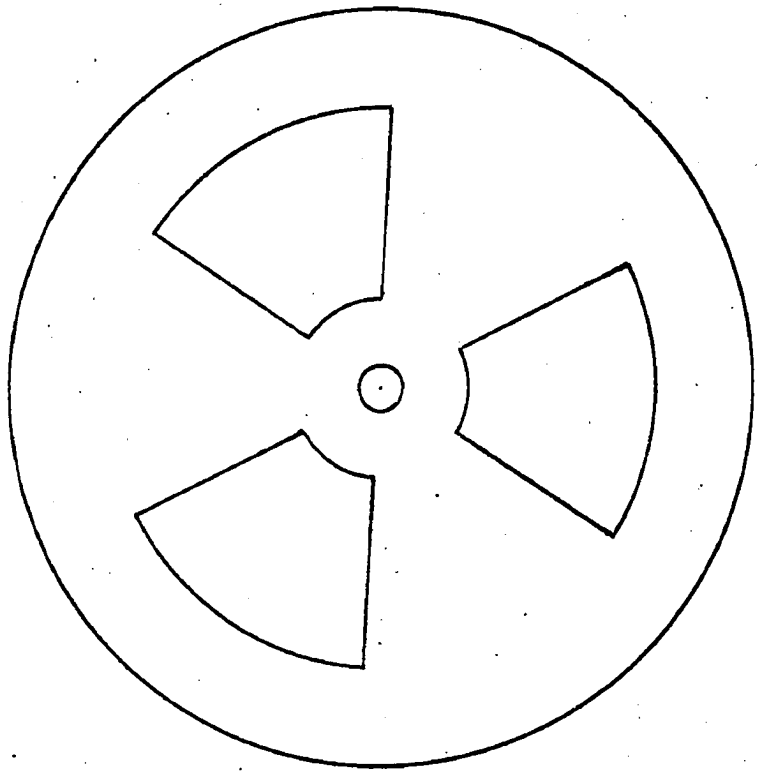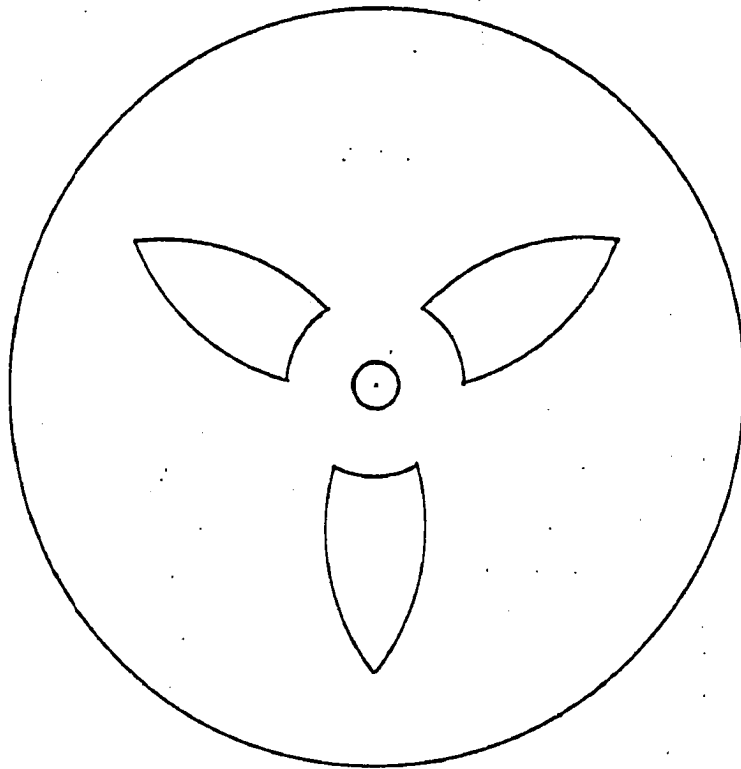
P_4 Baffle

(c)

and

$$\frac{N(P_4)}{N(P_0)} = \frac{\int_{\alpha_1}^{\alpha_2} Q(\alpha)\, P_4(\cos\alpha)\, \sin\alpha\, d\alpha}{\int_{\alpha_1}^{\alpha_2} Q(\alpha)\, \sin\alpha\, d\alpha} = f_4(\Omega^-) \quad (2.19)$$

where $N(P_2)$, $N(P_4)$, $N(P_0)$ are the respective count rates with the P_2, P_4 and P_0 baffles in place.

(iv) A Final Note

It is noted here that the angular correlation function is often written as follows:

$$W(\Theta) = 1 + f_2\, G_2\, A_2\, P_2(\cos\Theta) + f_4 G_4\, A_4\, P_4(\cos\Theta) \quad (2.20)$$

where G_2 and G_4 are attenuation factors. In the case of $\beta - \Omega^-$ correlations there are three possible kinds of attenuation-mechanisms, namely, after-effects of K - hole formation, electron straggling and static quadrupole interaction [Gerholm, Holmberg, Petterson, (unpublished)]. For the experiment in Au^{198} to be described, it was found by the above authors that G_2 and G_4 are essentially unity.

CHAPTER III

THE BAFFLE SYSTEMS

(i) The Gerholm Instrument

The spectrometer used in this experiment is due to T. R. Gerholm (1961). Magnetic momentum selection is provided in the electron channel which consists of an iron incapsuled long lens beta ray spectrometer with "triangular field" focussing. The instrument is a modification of the electron-electron coincidence spectrometer earlier developed by Gerholm.

Figure 3.1 (a) is a schematic of the $e^- - e^-$ spectrometer, whereas Figure 3.1 (b) is a schematic of the $e^- - \gamma$ spectrometer.)

The "triangular field" distribution is depicted in Figure 3.2. Magnetic field measurements [Gerholm, (1961)] show that the source is in a field free region and that the strength of the magnetic field increases roughly proportional to the distance from the source, when measured along the axis of symmetry.

(ii) Ring Focus and Baffles

In a lens spectrometer, the electrons leaving the source at an entrance angle α to the axis eventually return to the axis again to form an image. The spherical aberration of this image is large for many field shapes. A position of minimum spherical aberration generally occurs before the electrons cross the axis at the so-called ring focus (Figure 3.3). A great improvement in performance is obtained by placing the defining baffles at this focus rather than at the detector [Nichols, (1954)]. Ring focussing is employed in the Gerholm instrument.

Figure 3.1(a) Electron - Electron Spectrometer

Figure 3.1(b) Angular Correlation Spectrometer
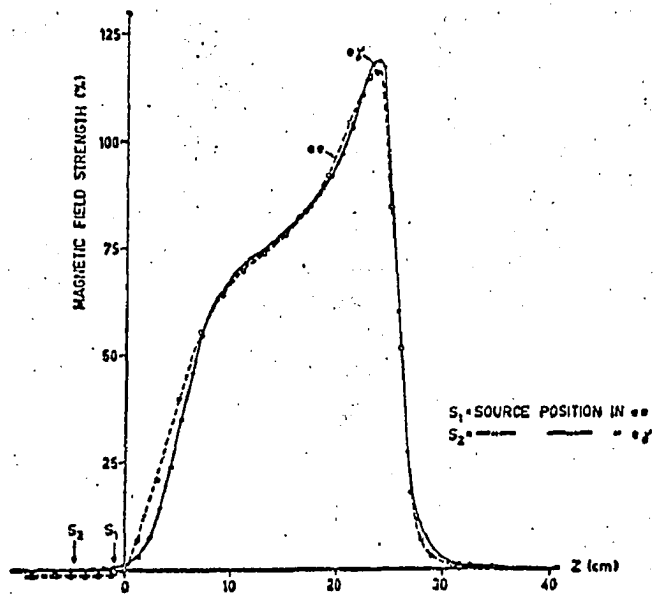
Figure 3.2   Triangular field distribution.
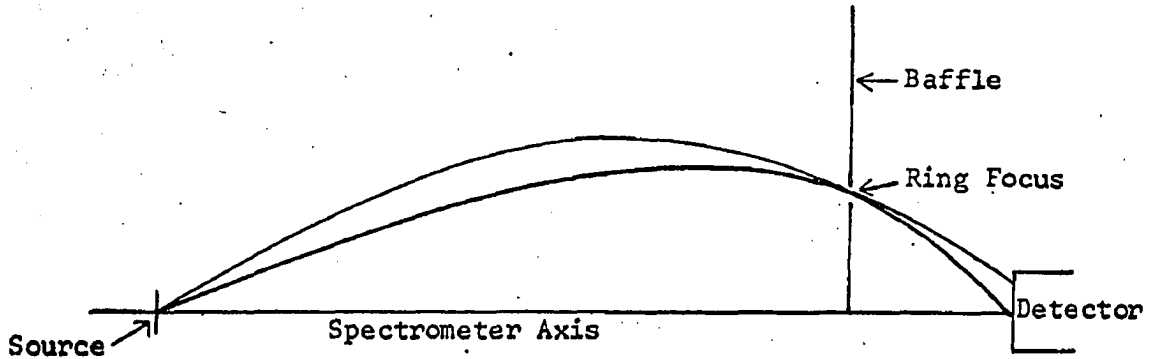
Figure 3.3   Ring Focus

(iii) Resolution and Transmission

The resolution of a spectrometer is usually determined by observing its response to a source of mono-energetic electrons. When the counting rate is plotted as a function of the magnetic field B, or the momentum p, one obtains response curves of the type shown below (Figure 3.4):
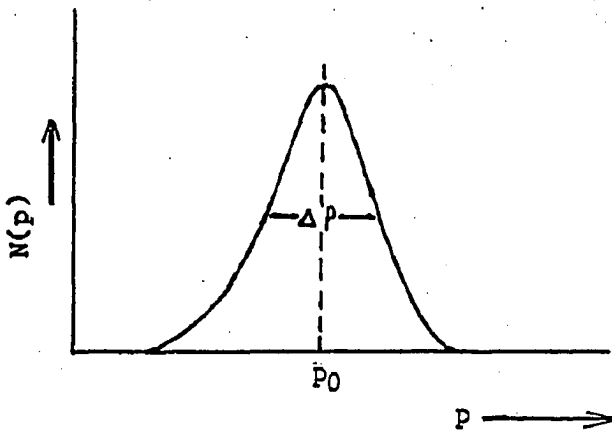
Figure 3.4

The resolution R is defined as ($\Delta p / p_0$) where Δp is the momentum spread at half maximum and p_0 is the momentum at the peak counting rate. R is independent of p_0. It should be noted that each instrument has its own characteristic line profile determined by its own particular focussing properties, but this definition of R can be used for all of them.

The transmission ω of a spectrometer is defined as the

fraction of the electrons of momentum p emitted from the source which arrive at the detector when the instrument is focussed on p. The expression ($d\Omega / 4\pi$), where $d\Omega$ is equal to the solid angle subtended by the baffle system, is a good approximation of ω.

(iv) The A_2 and A_4 Baffle Systems

(a) Special Remarks

The resolution of a magnetic spectrometer is essentially determined by three factors: the width of the source, the spherical aberration, and the width of the defining exit slit (generally the annular ring focus exit). If we neglect the width of the source and the spherical aberration the resolving power is determined solely by the width of the exit slit. Under these approximations the transmission increases proportional to $\sin \alpha$, α being the mean emission angle. Thus, the figures of merit of a magnetic spectrometer would seem to increase with increasing emission angle. The gain in transmission at a given resolution is, however, counterbalanced by an increased spherical aberration. If the spherical aberration is taken into account, the transmission $\omega(\alpha)$ considered as a function of the emission angle α has a maximum for a certain value of α which, of course, should be taken as the most favourable choice for the emission angle. It may be shown [DuMond, (1957)] that for a uniform field, $\omega(\alpha)$ has a broad maximum around 40° to 45°. Both theoretical and experimental studies of the "triangular field" show that its spherical aberration is somewhat larger than that of the uniform field and therefore $\omega(\alpha)$ in this case will have its maximum at a lower α-value. 30° should be close to the optimum value.

Thus, the net effect of the spherical aberration is to limit the mean emission angle and thereby the transmission (at a given resolution) to a certain maximum value. The shape of the field determines the most

favourable emission angle. The point to be noted then, is that the transmission (at a given resolution) is not a proper figure of merit for a directional correlation instrument. With increasing emission angle there will be a smearing out of the directional correlation owing to the finite aperture angle subtended by the accepted cone of electrons in the spectrometer.

Under normal circumstances the γ-correction factors $f_2 (\gamma)$ and $f_4(\gamma)$ are fairly close to unity and minor errors in these correct(γ) factors, therefore, do not seriously affect the experimental results.

The correction factors for the electron channel, however, decrease rapidly with increasing emission angle. This implies, in the first place, that the experimentally measured effect becomes smaller and therefore more difficult to determine. The gain in statistical accuracy obtained as a consequence of higher transmission is in this way counterbalanced. Obviously, one should choose a value for the emission angle α which is the most favourable compromise between statistical accuracy $\left(\simeq \sqrt{(\omega (\alpha))} \right)$ and smearing out $\left(\simeq f_\ell (\ell^-, \alpha) \right)$. Secondly, the choice of a fairly large emission angle implies that $f_2 (\ell^-)$ and $f_4(\ell^-)$ will become rather small and the results, therefore, more sensitive to the uncertainty in $f_2 (\ell^-)$ and $f_4 (\ell^-)$.

(b) Choice of Emission Angle

The problem consists in finding the value for α which maximizes the expression $\left[\omega^{1/2} (\alpha) f_\ell (\ell^-, \alpha) \right]$. This expression rather than the transmission should be considered as the proper figure of merit for an electron-gamma directional correlation spectrometer. If we neglect the spherical aberration and the broadening caused by the width of the source, the transmission may be written $\left[\omega (\alpha) = const. \times \sin\alpha \right]$. If, further, we restrict ourselves to a small angular interval $\delta\alpha$ around the

mean emission angle α , the appropriate expression for $f_2 (\ell^-, \alpha)$ becomes:

$$f_2(\ell^-, \alpha) = P_2 (\cos \alpha) = \frac{3\cos^2 \alpha - 1}{2} \qquad (3.1)$$

Consequently, one has:

$$\omega^{1/2} f_2 = const. \, (3 \cos^2 \alpha - 1) \sqrt{\sin \alpha} \qquad (3.2)$$

which has a broad maximum around $\alpha = 21.4°$.

Similar considerations apply for the $f_4 (\ell^-)$ correction factor. This factor, of course, decreases more rapidly with ω and calls for an even smaller emission angle.

In the construction of an A_2 baffle system it is preferable to choose the emission angle so large that the P_4 contribution is more or less completely wiped out, i.e. $f_4 (\ell^-) \simeq 0$. In this way the A_2 coefficients can be accurately determined directly from anisotropy measurements. The A_4 contribution will give only a negligible contribution to the anisotropy. If necessary a minor correction can be applied [Petterson, Thun, and Gerholm, (1961)].

If one wishes, however, to determine the A_4 coefficient, use of the above A_2 baffle system is of no help whatsoever because of the large α value. Optimum conditions of operation for A_4 coefficient determinations are obtained for $\alpha = 12°$ maximizing the expression:

$$\omega^{1/2} f_4 = const. \, (35 \cos^4 \alpha - 30 \cos^2 \alpha + 3) \sqrt{\sin \alpha} \qquad (3.3)$$

In the following pages, we will describe the actual construction of the A_4 baffle system used in this experiment.

(v) A_4 Baffle Construction

In the case of non-homogeneous fields where the electron trajectories cannot be calculated, the correct design parameters of the

baffle system must be determined by photographic ray tracing, for a detailed knowledge of the electron trajectories is important.

(a) The Camera and Special Baffles

A special camera (Figure 3.5) was built in order to take photographs of the electron trajectories inside the spectrometer chamber. This camera consists of a brass plate, with edges A and B accurately parallel to each other, and four Al rods inserted in it. These rods are placed at each end on either side of a centre line and perpendicular to the plate. A plastic film holder (Polaroid Slide Mount #633) is inserted in place between the respective pairs of Al rods.

When the camera is properly placed, the edges A and B rest firmly in the vacuum chamber, and the axis of the spectrometer passes through the film (i.e. the film is mounted in an axial plane (Figure 3.6)).

In taking an actual photograph, X-ray film was carefully cut and mounted in the film frame. Proper fiducial marks were made in order to determine its exact location in the spectrometer chamber.

In addition to the camera, 4 special Al baffles were constructed (Figure 3.7). These baffles have annular slits defining the electron emission angles to the range 12° to 18.5°. The mean emission angle and the transmission of each baffle are indicated in Table I.

TABLE I

Baffle	Mean Emission Angle	Transmission
I	13.0°	0.5%
II	15.3°	0.5%
III	17.5°	0.5%
IV	15.1°	1.5%

Film Holder ⟶   Al Rods⟶

A   B

Brass Plate

Figure 3.5   The Camera

Film ⟶

⟶ Spectrometer
Axis   ⟵Spectrometer
                              Chamber Wall
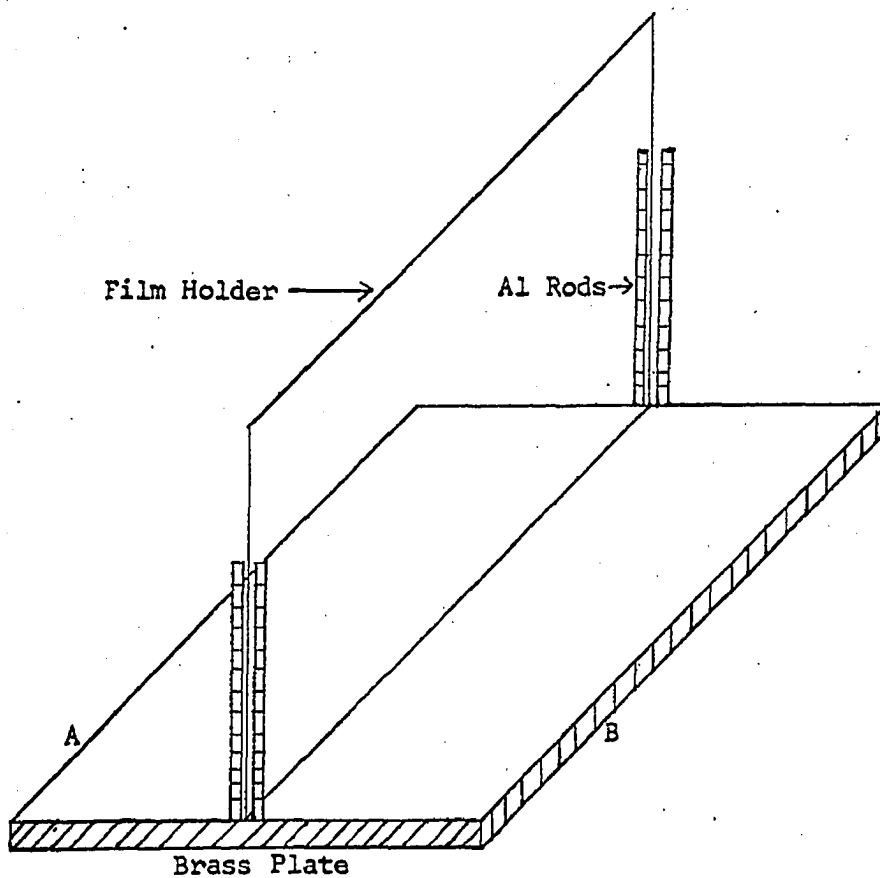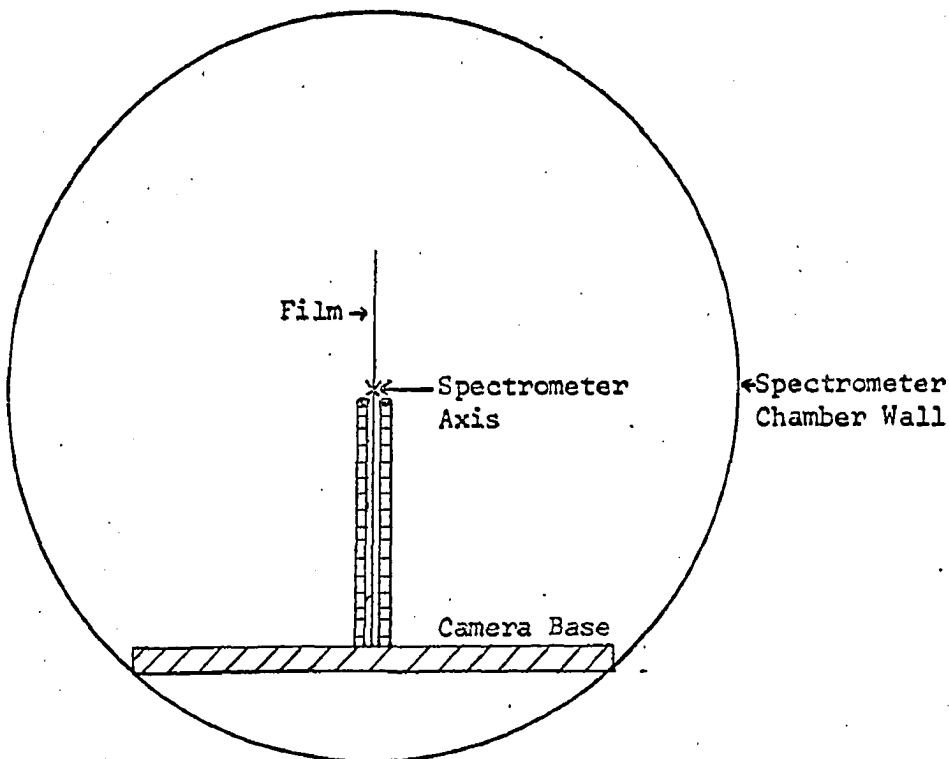
Camera Base

Figure 3.6   A front view of camera in spectrometer.
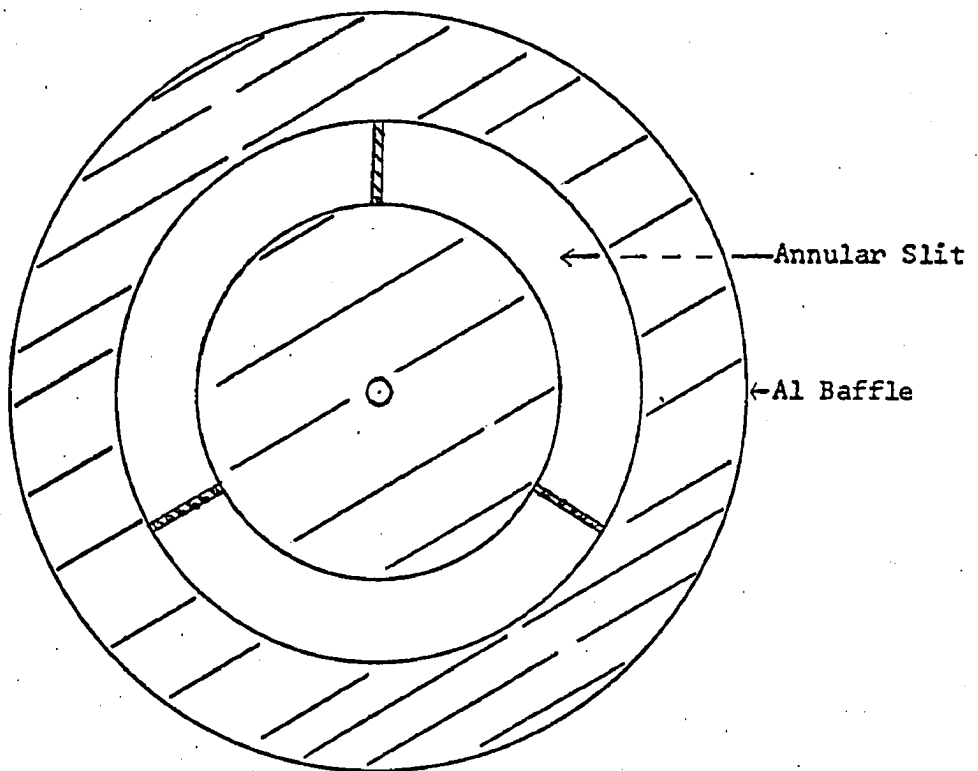
Figure 3.7   Al baffle with annular slit.

(b) The Photography

A Cs^{137} source was used in the ray tracing experiments. Using baffle IV (for maximum transmission) the 662 Kev conversion line of Cs^{137} was focussed in the spectrometer. The current setting for focussing was recorded and all photographs were taken at this current setting. In using any particular baffle, such baffle was placed perpendicular to the axis at the entrance of the spectrometer.

Photographs of the electron trajectories were taken with the entire series of baffles. Prints of these photographs are shown in Figure 3.8. Since the electrons describe spiroidal paths in the magnetic field they impinge at the sensitive surface of the film. After exposure and processing the film gives a picture of the electron trajectories as they would appear in a meridianal plane revoling with the electrons around the axis of symmetry. From these photographs it was decided that a mean emission angle much less than 15° would make the construction of the A_4 baffle system impractical. Hence a mean emission angle of approximately 15° was adopted for the A_4 baffle system rather than the optimum angle of 12°.

In Figure 3.9 we have an enlarged print of a photograph taken with baffle IV in place. A similar photograph was used to determine the dimensions of the A_4 baffle system. The ring focus is located in the region of maximum intensity on the photograph.

A superposition of photographs I, II and III was made in order to determine the upper and lower defining edges of the exit slit. Upon analysis of the photographs, the A_4 baffle system was constructed to fit the profile of the K - line. A schematic of the baffle is shown in Figure 3.10.

I

Figure 3.8
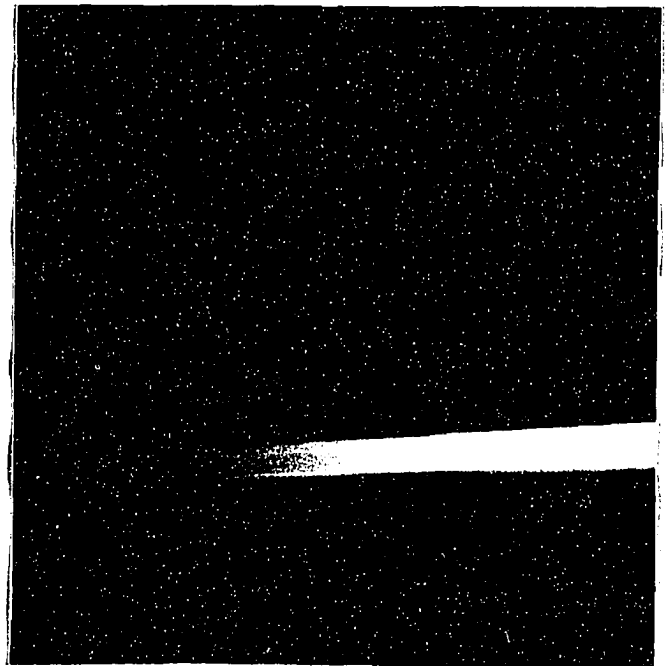
II

III

Figure 3.8
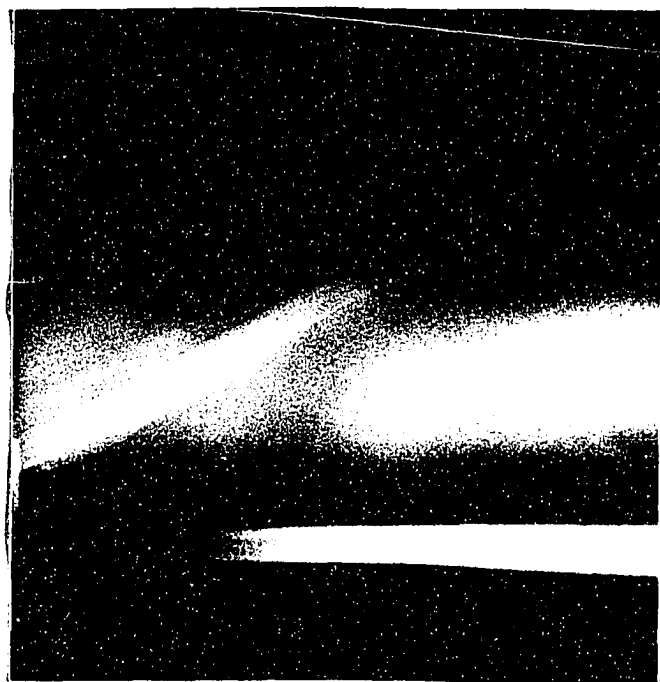
IV

Figure 3.9   An enlarged print.

Entrance Baffle

Exit Baffle

Ring

Lead Core
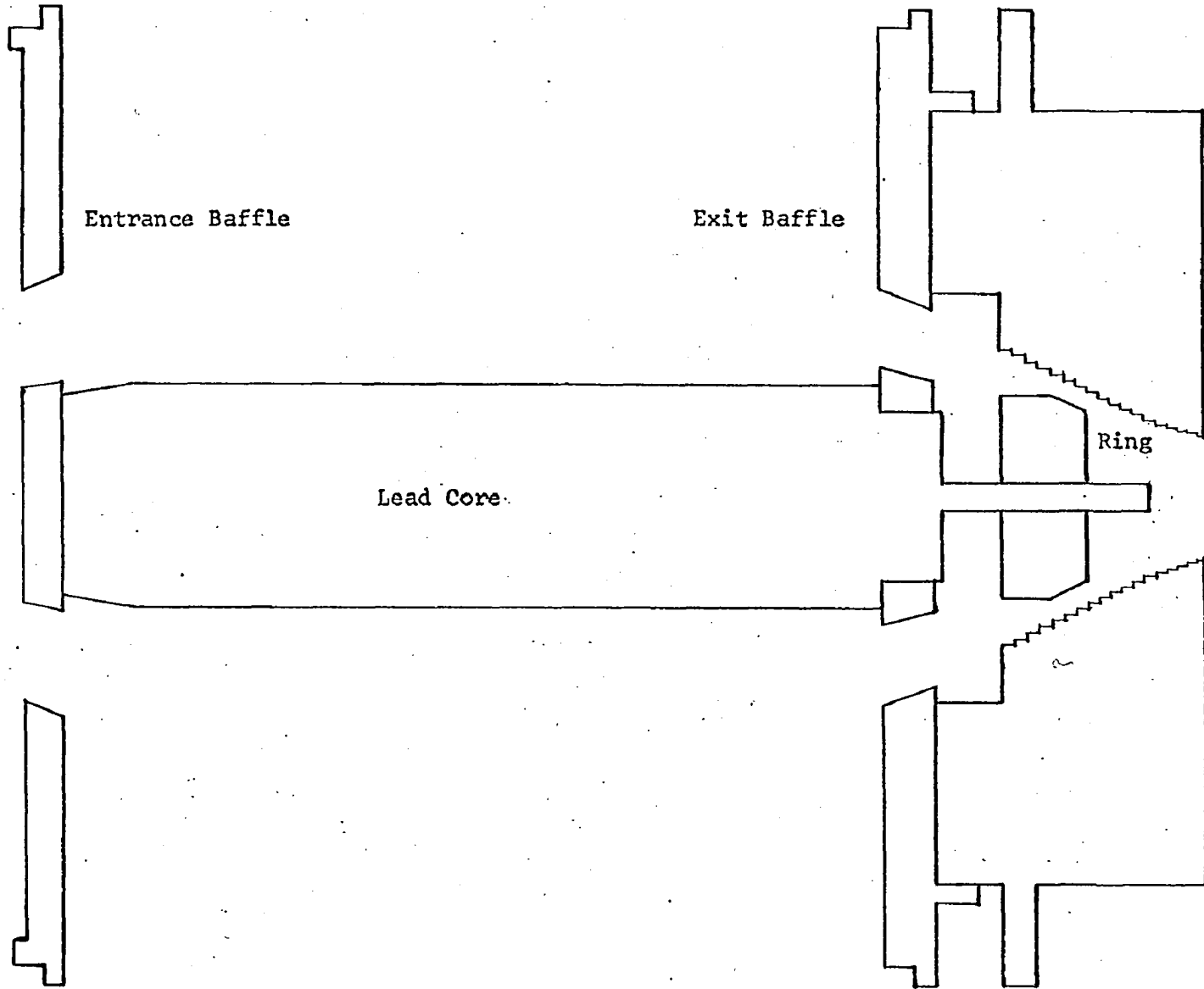
Figure 3.10   A schematic (side view) of the Al A_4 baffle system.

(c) The P_4 Baffle

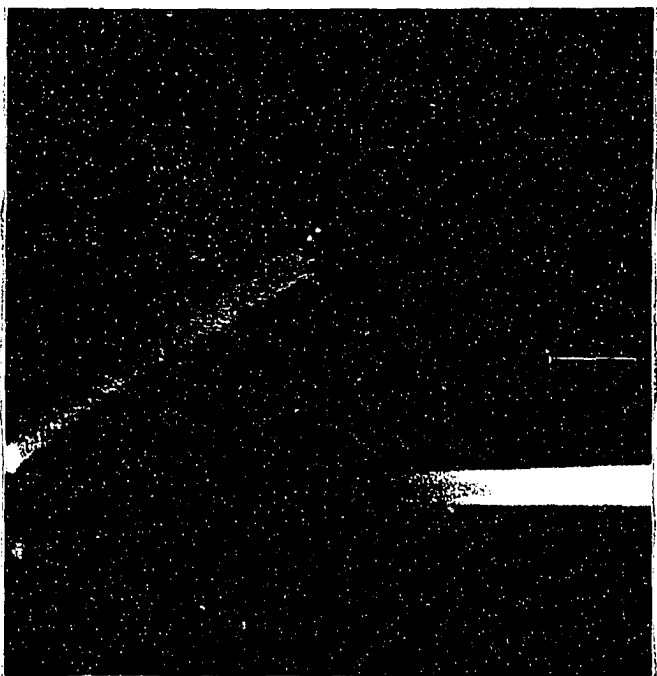The construction of the A_4 baffle system necessitated the construction of a P_4 baffle as well, in order to determine the correction factor $f_4(\varrho^-)$. Since this baffle had to be normalized relative to the P_0 baffle, a point by point plot of the P_4 baffle was imperative. This was accomplished by writing up a suitable computer program for the description of the P_4 baffle. This program was fed into the 1620 - II I. B. M. computer at the University.

The results of the program were utilized to plot the profile (c.f. Figure 2.6) of the P_4 baffle. It was found that the P_4 baffle profile corresponded exactly to the arc of a circle of radius 1.725". This latter fact enabled the construction of the P_4 baffle to proceed with relative ease.

CHAPTER IV

PRELIMINARY TESTING OF THE BAFFLES

(i) The A_4 -Baffle System

(a) Shadow Effect

The central part of the baffle system is supported by six legs. Three of them in the entrance end and three placed near the ring focus. It is possible to adjust the angular setting of the entrance and exit legs such that their shadows overlap. Thus there are effectively only three legs.

In this experiment the A_4 baffle system was tested for the shadow effect. This was accomplished as follows: the Cs^{137} 662 Kev conversion line was scanned in the beta-spectrometer with the entrance baffle set at vaious angles of rotation with respect to the exit baffle which was held fixed. The relationship between peak counting rate and angle setting was observed. The entrance baffle was then permanently fixed in that position which was found to correspond to the maximum peak counting rate.

(b) Resolution vs Transmission

The resolution and transmission of the A_4 baffle system for different "turns open" of the end ring were determined with the 662 Kev conversion line of Cs^{137}. The profiles obtained at different "turns open" are indicated in Figures 4.1 (a) and 4.1 (b).

From these profiles, values of resolution vs transmission were obtained. These values are listed in the following table:

44

counts/10 sec.

5 - 6 Turns Open

6 - 7 Turns Open

7 - 8 Turns Open

8 - 9 Turns Open

9 - Full Open

Spectrometer Current Setting
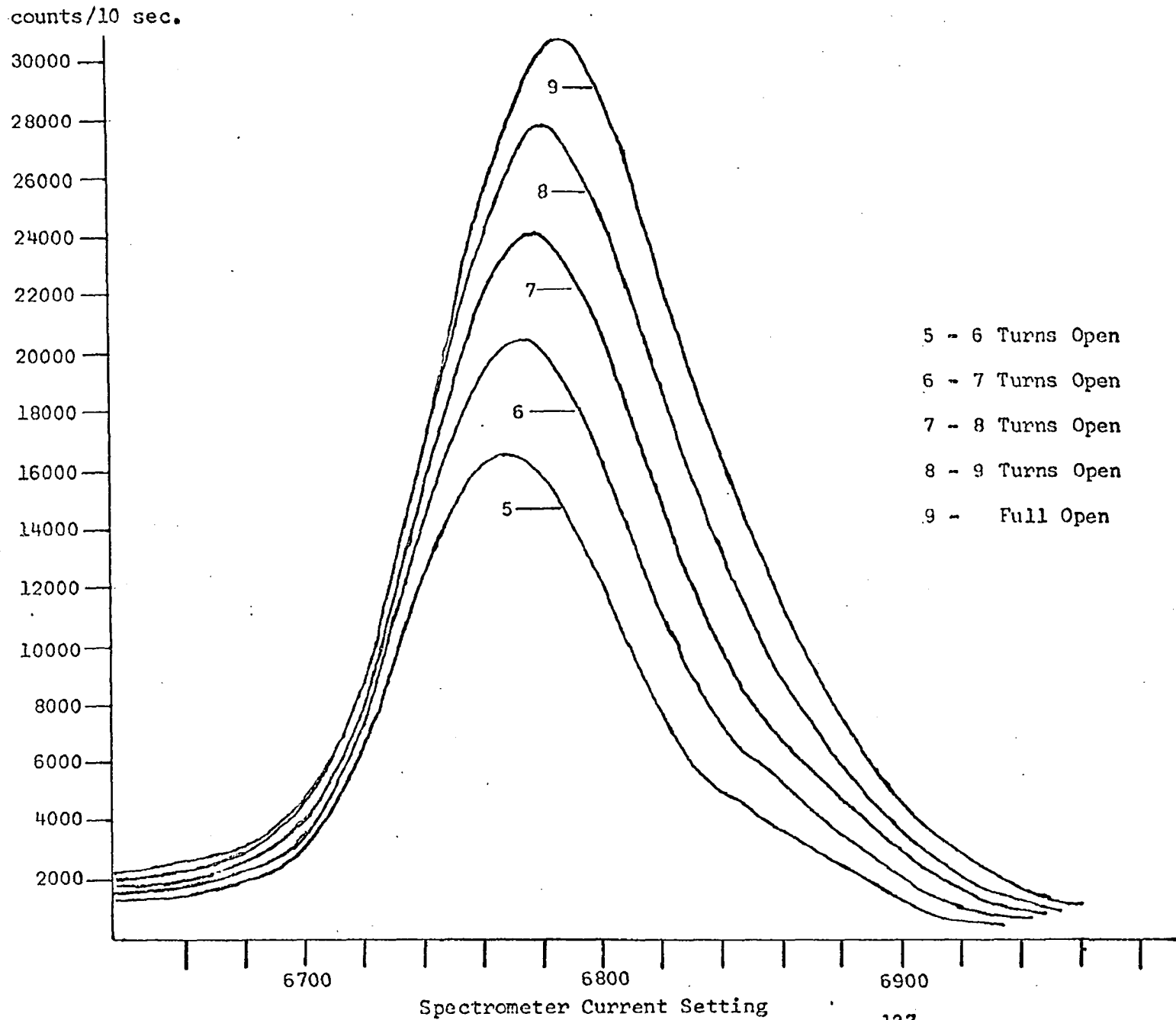
Figure 4.1(a)   Profiles of the 662 Kev conversion line of Cs^{137}.

counts/10 sec.

1 - 2 Turns Open

2 - 3 Turns Open

3 - 4 Turns Open

4 - 5 Turns Open

Spectrometer Current Setting
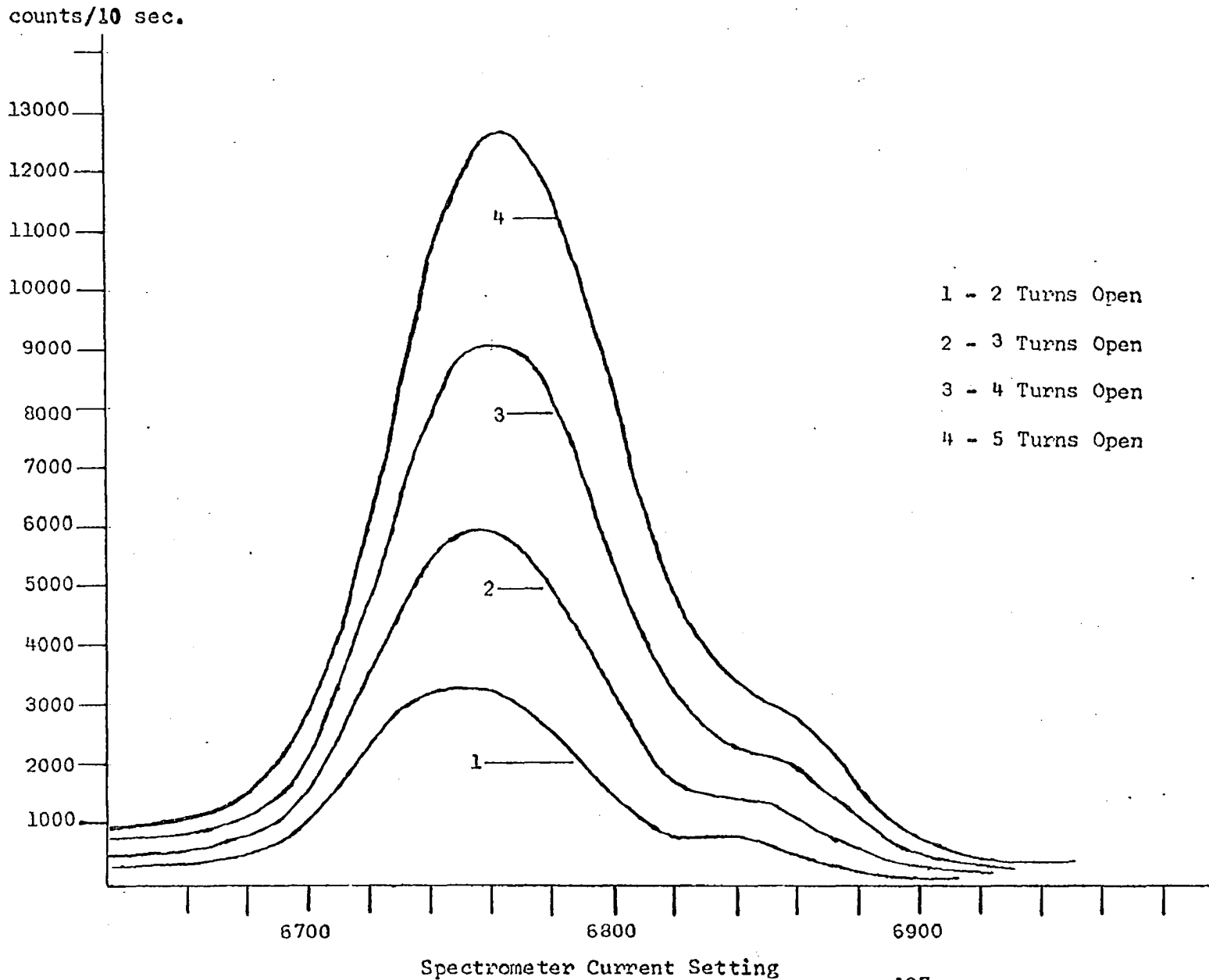
Figure 4.1(b)   Profiles of the 662 Kev conversion line of Cs^{137}.

TABLE II

Turns Open	Resolution ($\Delta p/p_0$)	Transmission (ω)
2	3.9%	0.2%
3	4.0%	0.3%
4	4.0%	0.5%
5	4.0%	0.6%
6	4.1%	0.8%
7	4.2%	1.0%
8	4.4%	1.2%
9	.4.5%	1.3%
Full Open	4.6%	1.5%

The values of the transmission were found as follows: with the baffle system "full open" the transmission, defined as $d\Omega/4\pi$ is 1.5%. This value of ω is determined by the annular slit width of the entrance baffle. Since the transmission is proportional to the solid angle $d\Omega$ subtended at the exit end of the baffle, and since the counting rate is also proportional to $d\Omega$, ω was calculated in the following way:

$$\omega = \frac{\text{Peak counting rate at a given "turns open" x 1.5}}{\text{Peak counting rate at "full open"}} \qquad (4.1)$$

Upon examining the above profiles and resolution-transmission values, it was decided to conduct the Au^{198} experiment at 6 "turns open".

(ii) Testing of the P_4 Baffle

Inasmuch as there was very little published information pertaining to the construction of the P_4 baffle, it was imperative that it be tested as soon as possible, and its performance compared to theoretical calculation. In the Au^{198} experiment to be described in the next chapter, the 412 Kev K - conversion line of Au^{198} was observed in the beta spectrometer, and the ratios [$N(P_2)$ / $N(P_0)$] and [$N(P_4)$ / $N(P_0)$ were

determined experimentally. The results were:

$$f_2(\ell^-) = \frac{N(P_2)}{N(P_0)} = 0.908 \pm 0.013$$

$$f_4(\ell^-) = \frac{N(P_4)}{N(P_0)} = 0.686 \pm 0.010$$

Since the transmission was $< 1\%$ the experimental values of $f_2(\ell^-)$ and $f_4(\ell^-)$ should have approximated very closely the P_2 and P_4 Legendre polynomials respectively, (cf. Chapter II) calculated at the mean emission angle of $15.1°$, i.e.

$$\left.\begin{array}{l} f_2(\ell^-) = P_2 \ (\cos \alpha) \\ f_4(\ell^-) = P_4 \ (\cos \alpha) \end{array}\right\} \qquad \alpha = 15.1°$$

A calculation of P_2 ($\cos 15.1°$) and P_4 ($\cos 15.1°$) yields:

$$P_2 \ (\cos 15.1°) = 0.900$$

$$P_4 \ (\cos 15.1°) = 0.682$$

The experimentally determined values of $f_2(\ell^-)$ and $f_4(\ell^-)$ therefore correspond to the theoretical values within the limits of error. This result was indeed expected for $f_2(\ell^-) = N(P_2) \ / \ N(P_0)$ since the performance of the P_2 and P_0 baffles has long been established in this laboratory. The correspondence between $f_4(\ell^-)_{expt.}$ and $f_4(\ell^-)_{theor.}$ however, proves conclusively that the P_4 baffle was properly constructed and that it is a reliable piece of equipment.

It is noted here that an error in the $f_2(\ell^-)$ and $f_4(\ell^-)$ determinations may be introduced as a result of the shadow of the three exit legs. The most correct method to measure $f_2(\ell^-)$ and $f_4(\ell^-)$ is:

$$f_2(e^-) = \int N_{P_2}(\varphi)\, d\varphi \Big/ \int N_{P_0}(\varphi)\, d\varphi \qquad (4.1)$$

$$f_4(e^-) = \int N_{P_4}(\varphi)\, d\varphi \Big/ \int N_{P_0}(\varphi)\, d\varphi \qquad (4.2)$$

where φ represents the angle of rotation of the P_0, P_2, and P_4 baffles

with respect to the fixed entrance baffle, and $N_{P_0}(\varphi)$, $N_{P_2}(\varphi)$ and

$N_{P_4}(\varphi)$ represent the peak counting rates at the angle φ. This is,

however, a tedious procedure and according to Gerholm (1961) the

formulae given above are sufficiently accurate provided the P_0, P_2

and P_4 baffles are placed such that there is no shadow of the rear legs

in the three "windows". Due to the rotation of the electron trajectories,

this means that the windows should be rotated somewhat with respect to

the entrance legs. Provided this is done the angular setting of the

baffles is not critical. The above procedure was followed in the

experimental determination of $f_2(e^-)$ and $f_4(e^-)$.

THE $_{79}$ Au ^{198} EXPERIMENT

(i) Introduction

Figure 5.1 shows the main modes of decay of the Au^{198} isotope. It has only one gamma - gamma cascade, viz, the 679 Kev γ - 412 Kev β cascade. In this chapter a gamma-electron directional angular correlation experiment to obtain the A_4 (γ e^-) and A_2 (γ e^-) correlation coefficients of the 679 Kev γ - 412 Kev e^- cascade is described. The b_2 and b_4 particle parameters are then calculated from these values and the tabulated values of A_2 (γ γ) and A_4 (γ γ) [Biedenharn and Rose, (1953)].

This experiment has been performed before [Gerholm, (unpublished)]. However, the main objective of the experiment is to indicate a new experimental technique for the study of the internal conversion process, and to assess the performance of the newly constructed A_4 baffle system.

(ii) Preparation

(a) Source Preparation

The source material was obtained in the form of irradiated gold foil. The gold was irradiated at McMaster University. It had an initial specific activity of 50 mc. / mg. A 5 mm. in diameter strip of this gold was glued onto a 0.00035" Al backing. This in turn was glued to an Al ring constructed so as to fit into the instrument source holder. This was then mounted in the Gerholm instrument. The source was centered by focussing the 412 Kev K - conversion line of Au^{198} (Figure 5.2) in the beta spectrometer.

(b) Gamma Probe Centering

Two gamma probes utilizing NaI crystals were used independently in the experiment. These probes were centered by comparing the "γ-singles" count rates at various angles of the probe. The first probe, denoted γ-1 ,
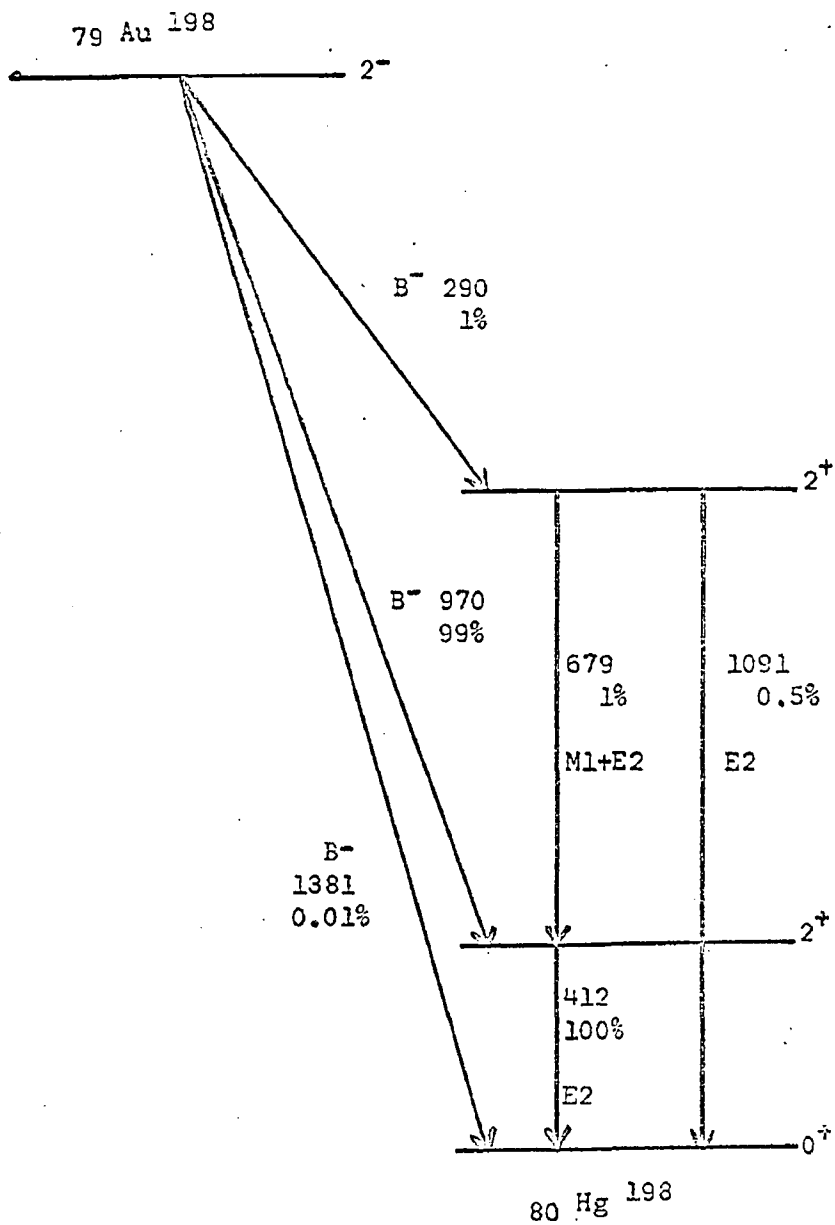
50

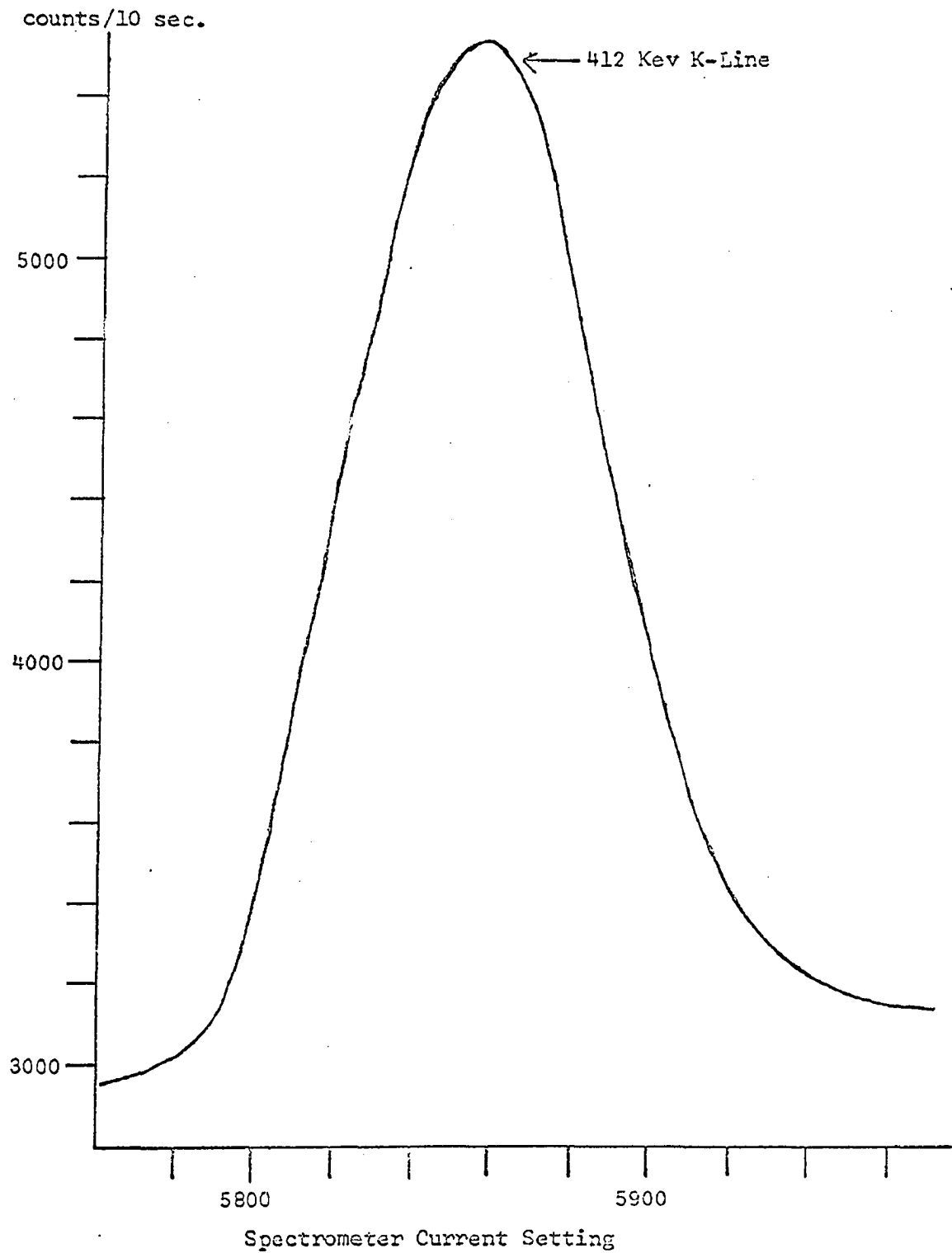Figure 5.1   The Au^{198} Decay Scheme.

counts/10 sec.

412 Kev K-Line

5000

4000

3000

5800

5900

Spectrometer Current Setting

Figure 5.2   412 Kev conversion line of Au^{198}.

was set at angles of 180°, 225° and 270°; the second probe, denoted γ-2,
was set at angles of 90°, 135° and 180°.

(c) The Spectrometer Settings

The gamma spectrometers were finally fixed in position so
that the face of each scintillator crystal was 10 cm. from the source.
The γ-1 probe utilized a 2 x 2" crystal whereas the γ-2 probe utilized a
1 3/4 x 2" crystal.

The A_4 baffle opening was set at 6.0 turns open. A plastic
scintillator in the beta spectrometer was used as the conversion electron
detector.

(d) The Experimental Arrangement

Figure 5.3 shows a block diagram of the circuit layout used
for the γ-2 angular correlation experiment.

The outputs of the detectors are divided into a slow and fast
channel. The slow channels using linear amplifiers contain the pulse
height information. In the fast channels, only the very first part of
each pulse is used. This leading edge is shaped into a very short pulse
($\simeq 10\ m\,sec.$) with delay lines. The width of these pulses essentially
determines the resolving time of the circuit. The fast circuit gives
an output for γ_1-e^- and γ_2-e^- coincidences but not for γ_1-γ_2 coincidences
(Figure 5.4). The outputs of the two slow channels and of the fast
coincidence circuit are fed into two slow triple coincidence circuits.
The outputs of these slow coincidence circuits and of the single channel
analysers are recorded in scalers.

The gamma-electron directional correlation was fully
automated [Young, (1965)]. A detailed description of the electronics
described above has been given by Colclough (1963) and Young (1965), and
may be referred to for further information.
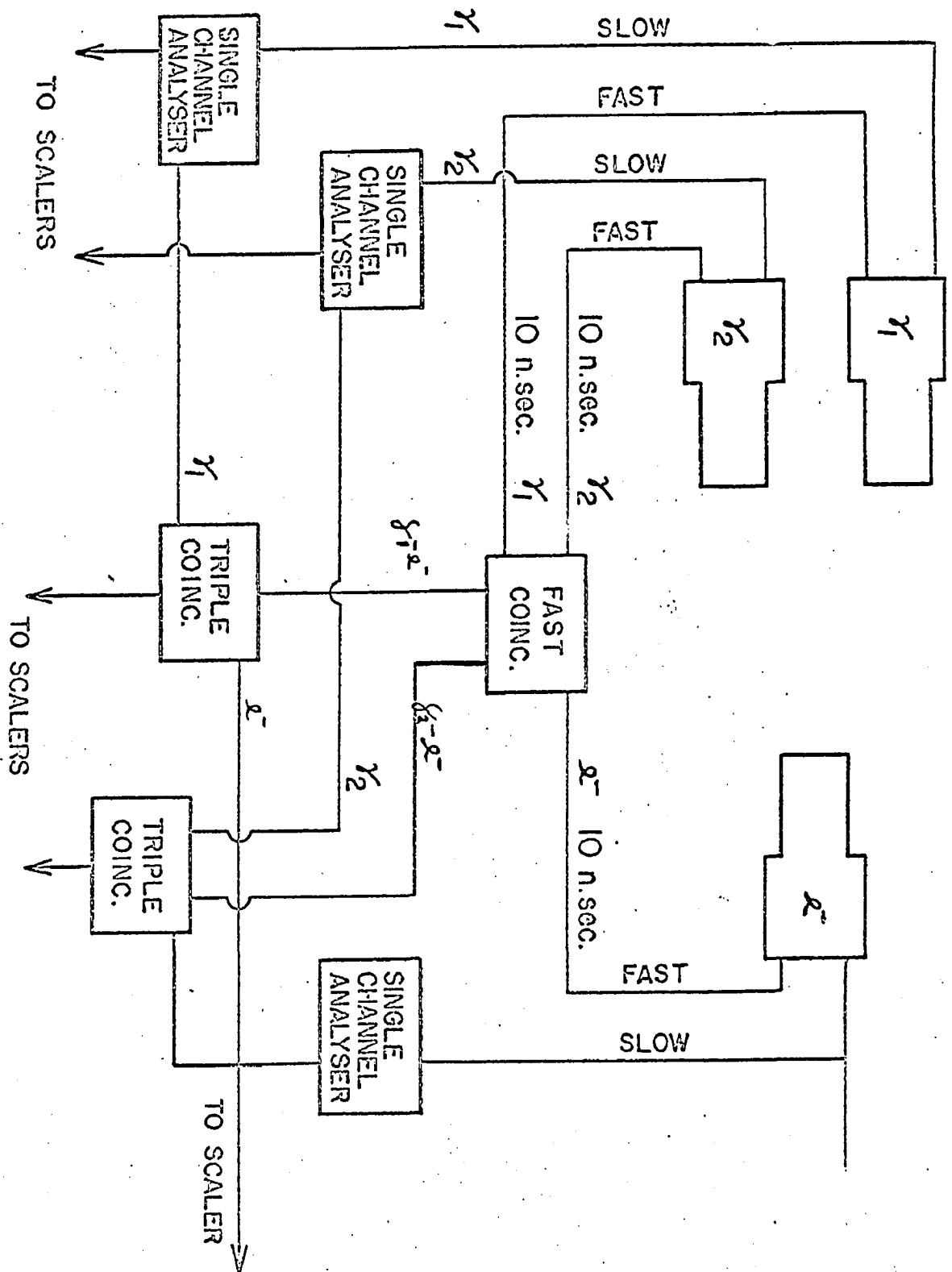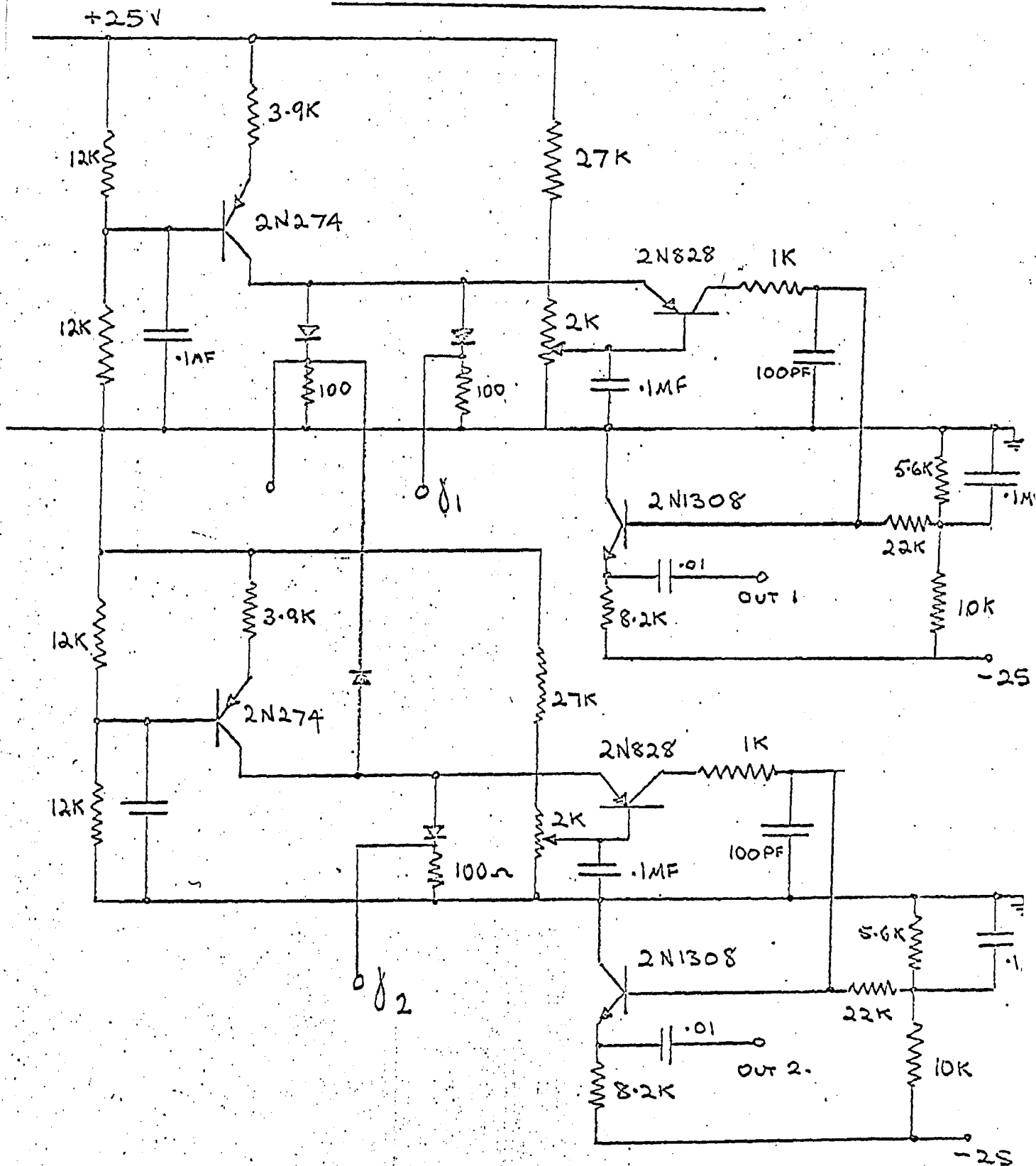
Figure 5.3 A Block Diagram of Circuit Layout

Figure 5.4 A Two Fold Fast Coincidence Circuit

(iii) Experimental Procedure

The $f_2(e^-)$ and $f_4(e^-)$ correction factors were determined experimentally using the 412 Kev K - conversion line of Au^{198}. The results were:

$$f_2(e^-) = 0.908 \pm 0.013$$
$$f_4(e^-) = 0.686 \pm 0.010$$

The γ-spectrometers were then set to accept the 679 Kev gamma photopeak (Figure 5.5). This energy setting, however, was located on the tail of the strong 412 Kev gamma photopeak (Figure 5.5) and so β^-- 412 Kev gamma coincidences appeared as background.

The beta spectrometer was set on the peak of the 412 Kev K-line (Figure 5.2) and coincidences were recorded with the gamma spectrometers at the angles 180°, 225°, 270° for γ-1, and 90°, 135°, 270° for γ-2.

The beta spectrometer was then set off the peak of the 412 Kev K-line and the background coincidences were recorded at the above angles.

The chance (accidental) coincidence counting rate was determined under each set of conditions. This was accomplished by delaying the β^- pulses from the beta spectrometer by means of a delay line cable.

(iv) Treatment of Data and Calculations

The data was corrected for chance and decay of the source, and normalized to the single channel counting rates. The genuine coincidence rate at each angle was then determined by subtracting the corrected "OFF PEAK" data from the corrected "ON PEAK" data. A summary of the results are shown in Table III for each γ-e^- correlation angle.

The uncorrected values of $A_2(\gamma e^-)$ and $A_4(\gamma e^-)$ were obtained by solving the equation:

TABLE III

$\gamma - \ell^-$ Correlation Results

(I) For the γ -1 Probe

Angle	On Peak Counts	Off Peak Counts	Genuine Counts
180°	3765 ± 61	2317 ± 48	1448 ± 78
225°	4478 ± 67	2368 ± 49	2110 ± 83
270°	4565 ± 68	2128 ± 46	2437 ± 82

A_2 $(\gamma \ell^-) = - 0.27 \pm 0.03$ } Uncorrected for Finite

A_4 $(\gamma \ell^-) = + 0.07 \pm 0.04$ } Solid Angle

(II) For the γ -2 Probe

Angle	On Peak Counts	Off Peak Counts	Genuine Counts
180°	6110 ± 78	4452 ± 67	1658 ± 103
135°	6383 ± 80	4402 ± 66	1901 ± 104
90°	6782 ± 82	4269 ± 65	2513 ± 105

A $(\gamma \ell^-) = - 0.29 \pm 0.04$ } Uncorrected for Finite

A $(\gamma \ell^-) = + 0.06 \pm 0.04$ } Solid Angle

Figure 5.5   The 412 Kev and 679 Kev photopeaks.

$$W(\Theta) = 1 + A_2 \left(\gamma \, e^- \right) P_2 (\cos \Theta) + A_4 \left(\gamma \, e^- \right) P_4 (\cos \Theta) \qquad (5.1)$$

at all angles for each gamma probe γ-1 and γ-2. These values are tabulated

in Table III. The values of $A_2 \left(\gamma \, e^- \right)$ and $A_4 \left(\gamma \, e^- \right)$ corrected for finite

solid angle along with the values of f_2 and f_4 are tabulated in Table IV.

The mean values obtained were:

$$A_2 \left(\gamma \, e^- \right) = - 0.32 \pm 0.02$$

$$A_4 \left(\gamma \, e^- \right) = + 0.10 \pm 0.04$$

The values of the A_2 and A_4 coefficients and of the b_2

particle parameter obtained by Gerholm (unpublished), which are in

agreement with the theoretical values of Biedenharn and Rose (1953), are

listed in Table V.

Utilizing the values of $A_2 \left(\gamma \, \gamma \right)$ and $A_4 \left(\gamma \, \gamma \right)$ from Table V

and our experimental values of $A_2 \left(\gamma \, e^- \right)$ and $A_4 \left(\gamma \, e^- \right)$ we obtain:

$$b_2 = \frac{A_2 \left(\gamma \, e^- \right)}{A_2 \left(\gamma \, \gamma \right)} = 1.19 \pm 0.15$$

$$b_4 = \frac{A_4 \left(\gamma \, e^- \right)}{A_4 \left(\gamma \, \gamma \right)} = 0.53 \pm 0.26$$

Using the recursion formula for b_2 (Chapter I) we obtain:

$$b_2 = \frac{1.40 - b_4}{2.5} = 1.19 \pm 0.10$$

(v) Errors

The dominant experimental error was statistical in nature

and was due primarily to the low specific activity of the course.

(vi) Conclusions

The values obtained for the b_2 particle parameter indicate

that the new experimental method for the study of the internal conversion

TABLE IV

Probe	f_2	f_4	$A_2(\gamma\alpha^-)$ [Corrected]	$A_4(\gamma\alpha^-)$ [Corrected]
ϕ -1	0.875	0.608	$= 0.31 \div 0.03$	$+ 0.11 \div 0.06$
ϕ -2	0.883	0.626	$= 0.33 \div 0.04$	$\div 0.10 \div 0.07$

Mean Values: $A_2(\gamma\alpha^-) = - 0.32 \pm 0.02$

$A_4(\gamma\alpha^-) = \div 0.10 \pm 0.04$

Experimental Results

TABLE V

k	$A_k(\gamma\alpha^-)$	$A_k(\gamma\gamma)$	$b_k[A_k(\gamma\alpha^-)/A_k(\gamma\gamma)]$	b_k [From Formula]
2	$- 0.38 \pm 0.02$	$- 0.27 \pm 0.02$	1.41 ± 0.15	1.32 ± 0.04
4	$\div 0.04 \pm 0.02$	$\div 0.19 \pm 0.02$	0.20 ± 0.10	

Gerholm's Results

process yields an improved accuracy in the b_2 determination. A further merit of the method is seen in the fact that a reasonable value of b_2 is obtained from the recursion formula despite a somewhat large error in A_4.

Furthermore, it is concluded that the A_4 baffle system was properly constructed since the experimental determinations of the $f_2(\ell^-)$ and $f_4(\ell^-)$ correction factors agreed with the theoretical values. This agreement is contingent upon the proper construction of the A_4 system.

In future work involving the determination of particle parameters as well as of conversion coefficients the use of stronger sources seems strongly indicated.

BIBLIOGRAPHY

Arns, R.G. and Wiedenbeck, M.L. 1958. Phys. Rev. 111, 1631.

Biedenharn, L.C. and Rose, M.E. 1953. Revs. Modern Phys. 25, 729.

Church, E.L. and Weneser, J. 1956. Phys. Rev. 104, 1382.

Colclough, J.D. - Thesis, Assumption University of Windsor, (1963).

Coleman, C.F. 1958. Nuclear Phys. 5, 495.

Du Mond, J.W. 1957. Ann. Phys. 2, 283.

Ferentz, M. and Rosenzweig, N. 1955. AEC Report ANL - 5324.

Frauenfelder, H.F. 1955. in "Beta and Gamma Spectroscopy"
    (K. Siegbahn, ed.). p. 531, Interscience, N.Y.

Gerholm, T.R., Holmberg, L. and Petterson, B.G. (unpublished).

Gerholm, T.R. 1961. Ark. f. Fysik, 21, 253.

Gerholm, T.R. (unpublished).

Green, T.A. and Rose, M.E. 1958. Phys. Rev. 110, 105.

Nichols, R. and Jensen, E. 1954. Phys. Rev. 94, 369.

Petterson, B.G., Thun, J.E. and Gerholm, T.R. 1961. Nuclear Phys.
    24, 223.

West, H.I. 1959. U.C.R.L. 5451.

Young, R.H. - Thesis, University of Windsor, (1965).

VITA AUTORIS

1941 - born in Windsor, Ontario on December 8.

1960 - graduated from Corpus Christi High., Windsor, Ontario.

1963 - received Bachelor of Science in Physics, University of Windsor.
- entered the Faculty of Graduate Studies at the University of Windsor to proceed toward M.Sc. degree in Physics.